OPSIN DIVERSITY AND MOLECULAR CHARACTERIZATION OF THE PHOTOTRANSDUCTION CASCADE IN MODIFIED CRUSTACEAN EYE TYPES WITH A FOCUS ON *ALIMA PACIFICA*, *NEOCALANUS FINMARCHICUS*, AND *LABIDOCERA MADURAE*

A THESIS SUBMITTED TO THE GRADUATE DIVISION OF THE UNIVERSITY OF HAWAI'I AT MĀNOA IN PARTIAL FULFILLMENT OF THE REQUIREMENTS FOR THE DEGREE OF

MASTERS OF SCIENCE

IN

MARINE BIOLOGY

MAY 2016

By

Mireille Steck

Thesis Committee:

Megan Porter, Chairperson

Petra Lenz

Andy Christie

Keywords: Opsin, crustacean vision, phototransduction

ACKNOWLEDGEMENTS

I would first like to acknowledge my wonderful advisor, Dr. Megan Porter for taking me into her lab despite the challenging time constraints I had proposed for my project. Without her knowledge, infinite patience, fine editing skills, and coffee supply this thesis would not have been possible. My committee members, Dr. Petra Lenz and Dr. Andrew Christie, have been so helpful throughout this process and their willingness to help me on such short notice, for a project this in depth has been extremely appreciated. Other valuable brains were picked from PBRC, including Dr. Vittoria Roncalli and Mr. Matthew Cieslak – their responses to late night emails and calming words in several panicked meetings were crucial to the completion of this project, and no words can express my gratitude for the time they have given me.

In addition to the literary gems which have tended this thesis to fruition, I would also like to thank my emotional support team. Lauren Van Heukelem, who was always there to feed me and take me to algae collect when writing was too much to handle. Sean and Hoku for their unwavering support and many horrible break out room puzzles to take my mind off of science. My lab mates, Albert Chan and Sitara Palecanda for providing me with sugars and small talk whenever I was typing in/near the lab. The Tifts for always quietly supporting me and for taking care of Cheyenne as she grows old, particularly Auntie Sabine and Simone for keeping me company and feeding me in the fall of my endless programming challenges. Grandma Jhan for her infinite words of wisdom and wonderful care of my too many fish tanks while visiting. Auntie Ellen and my cousins, Alex and Jasmine, who have been here to listen to my practice talks, read random drafts full of jargon and give me way too many sweets. Uncle Allen and Auntie Liz for their support for the past seven years of undergraduate work *and* graduate work – life would have been much harder without our monthly dinners and occasional beach days. My sisters Katrina and Emily for the rejuvenating sister-talks we can only seem to have every six months. My amazing parents for supporting me through so many years of college both financially and emotionally – without you none of this would have been possible! And thank you for enduring my holiday Peeps®, despite the horrendous flavors I insisted on sending you as a stress relief– knowing you ate them out of love will always be a memory I cherish. And lastly to the love of my life, Kristianne Agusto, who has been with me through the many trials and tribulations of this process; for all the fish tank scrubbing, for all the late night powerpointing, and for always lending me an ear for a tirade or molecular babble. I would like to thank everyone from the bottom of my heart and know that none of this would have been possible without your presence, support, and food. Mahalo to everyone, and please enjoy reading about visual systems.

ABSTRACT

Evolution of the crustacean visual system is complex and cryptic; unusual eye types coupled with an abundance of visual pigments depicts a history of rapid diversification. Using transcriptomic analysis, visual phototransduction genes were identified from whole copepods of *Neocalanus flemingeri,* (naupliar eye), and *Labidocera madurae* (transformed naupliar eyes), and from the double retina compound eye of last-stage stomatopod larvae (*Alima pacifica*). Similar components to the visual phototransduction cascade of *Drosophila melanogaster* were identified in all species. Identified visual opsins clustered with long-wavelength sensitive, middle-wavelength sensitive (MWS) and ultraviolet sensitive opsins in *A*. *pacifica*, while both copepods expressed only MWS opsins. Non-visual pteropsins were identified in all three species, and one peropsin was found in *A. pacifica.* Developmental shifts in opsin expression of larval versus adult transcriptomes were identified in both *L. madurae* and *A. pacifica*. The molecular components of these unusual eye types supplement the history of crustacean visual evolution.

TABLE OF CONTENTS

List of Tables

List of Figures

Chapter 1:
Phototransduction in Crustaceans

The main goal of this thesis was to characterize the molecular components of phototransduction cascades in the unusual crustacean eye types of the stomatopod *Alima pacifica*, and the copepods *Labidocera madurae* and *Neocalanus flemingeri*. Crustaceans have a wide diversity of eye types when present, though these can be separated into two general groups: simple eyes (as seen in copepods) or compound eyes (as seen in stomatopods) (Cronin and Porter, 2008). The simple eye, also known as the naupliar eye, is comprised of only photoreceptor cells, often lacking lenses and crystalline cone structures. The compound eye is more complex, having ommatidial units composed of rhabdomeric photoreceptors, crystalline cone structures, and lenses. These ommatidial units can act independently, with single lenses focusing light onto single photoreceptors (apposition type eyes), or with multiple lenses working together to focus light onto a single photoreceptor (superposition type eyes).

The diversity of eye types found in crustaceans comes from modifications in the structures and variations in the arrangements of visual system components such as photoreceptors, lenses and crystalline cone structures within simple or compound eyes. Apposition compound eyes are the most common eye type in the crustaceans. In stomatopods, transformations of the basic apposition ommatidial design have resulted in the most complex set of photoreceptors characterized in any animal visual system (Marshall et al., 2007a). The eye of the adult stomatopod is divided into three lobes: a dorsal and ventral lobe composed of typical crustacean-type ommatidial units, and a midband row with enlarged lenses and subdivisions of photoreceptors in the first four rows (Marshall et al., 2007a). In contrast, the simple naupliar eye is present in only three crustacean groups: Copepoda, Ostracoda and Thoracica (Cronin and Porter, 2008). Of these groups, the copepods stand out due to a diversity of visual system arrangements, with multiple families having examples of modified naupliar eyes, often separating the three-lobes into three spatially separated eyes with lenses (Elofsson, 2006). The arrangement of photoreceptors in both stomatopod and copepod eyes are unusual when compared to those of other crustaceans, despite their differences in structural complexity.

Regardless of eye type, the phototransduction cascade that occurs within photoreceptors has molecular components which remain relatively conserved among taxa. Opsin proteins initiate phototransduction and are highly diversified within the crustaceans, an event not seen in many other

invertebrate groups (Porter et al., 2012). While some crustaceans, such as *Daphnia pulex* have been characterized from genomic analysis (Mahato et al., 2014), those with more unusual types of eyes remain largely uncharacterized. No previous molecular characterization of the unique visual systems of *Alima pacifica*, *Labidocera madurae,* or *Neocalanus flemingeri* has occurred, and the following thesis will focus on the discovery and characterization of phototransduction components in these species.

The primary objectives of this study were to 1) identify the molecular components potentially involved in phototransdcution cascades of three unusual crustacean eye types, 2) assess any developmental changes that may be present in the visual systems of these animals, and 3) identify differences in opsin diversity, in relation to eye complexity (Chapter 4). The first and second objectives represent independent studies for *Alima pacifica* (Chapter 2) and the Calanoid copepods (Chapter 3), and to accomplish these goals I used data generated by other researchers. Copepods were collected from the Gulf of Alaska (*Neocalanus flemingeri*) and Kaneohe Bay, HI (*Labidocera madurae*), and subsequently processed for sequencing by PBRC members, Dr. Petra Lenz and Dr. Vittoria Roncalli. Stomatopod last stage larvae, having the most complex eye, were collected by Dr. Megan Porter from coral reefs at the Lizard Island Research Station, Queensland, Australia. Sample processing and sequencing occurred in different facilities for the samples from each species.

The comparisons of molecular phototransduction components within each eye type, as well as among eye types, provided valuable insights into the evolutionary history of visual systems in crustaceans. Several new components of crustacean visual systems, such as non-visual opsin and copepod opsin diversity, were revealed by this research and will be discussed in greater depth in the following thesis.

Chapter 2:
Phototransduction in *Alima pacifica* late-stage larval double retinas: insights on eye development through transcriptomes

Introduction

There is no question that the eye types in arthropods are unique, varied, and often highly complex. The complexity of the arthropod eye has achieved its peak, however, in the exceptional eye of the stomatopod. These crustaceans have three visual fields within in a single eye (Marshall et al., 2007b) coupled with numerous spectral classes of photoreceptors (Cronin and Bok, 2014; Cronin and Marshall, 1989; Cronin and Porter, 2008; Cronin et al., 1996; Marshall et al., 2007b; Porter et al., 2010). The visual fields result from the subdivision of the stomatopod eye into a ventral and dorsal lobe, separated by a midband. The retina of a stomatopod has 16 different photoreceptor types which contribute to vision: twelve of these are involved in color vision, at least two are involved in polarization vision, with an additional two used for spatial vision (Marshall et al., 2007b). In the dorsal and ventral hemispheres, two types of photoreceptors are present: a distal R8 cell and an underlying ring of R1-7 cells which create a long, fused rhabdom. This general set up is very similar to that of other malacostracan crustacean eyes (Cronin and Porter, 2008). The mid-band row is where most of the retinular specialization occurs, containing the 14 remaining types of photoreceptors: rows 1-4 are host to the photoreceptors involved in color vision while rows 5 and 6 contain photoreceptors involved in polarization vision (Cronin and Porter, 2008; Marshall et al., 2007b). Typically, the ommatidial units in rows 1-4 exhibit UV sensitivity in the R8 photoreceptor unit, while the R1-7 cells have been subdivided and are each sensitive to different wavelengths of light (Marshall et al., 2007b). Rows 2 and 3 of the midband also possess colored filters between rhabdom tiers, which have a colored carotenoid-like substance that may be unique between species (Marshall et al., 2007b; Porter et al., 2010). Rows 5 and 6 have enlarged R8 cells when compared to the ommatidial units of the dorsal and ventral hemispheres, with microvilli arranged orthogonally in the R1-7 unit, and unidirectionally in the R8 rhabdomere (Cronin et al., 2010; Marshall et al., 2007b). The specialized photoreceptors of the midband are coupled with larger lenses, which allow for heightened sensitivity without any part of the eye becoming over- or under-exposed (Marshall et al., 2007b).

Yet the structural and spectral components of the eye are only a part of the visual complexity found in these animals. Little work has been done on the other molecular components involved in phototransduction of stomatopods, though transcriptomic analyses have suggested similar signaling

components to the visual cascades present in *Drosophila melanogaster* exist (Porter et al., 2013). In this cascade, opsin proteins initiate intracellular signaling using G-proteins, trp calcium ion channels and arrestins to regulate activity (Katz and Minke, 2009). Opsin diversity is extensive among metazoan taxa, though these proteins evolutionarily cluster into four main clades (Henze and Oakley, 2015; Porter et al., 2012); the following will discuss the three groups that are relevant to crustacean vision. C-type opsins are generally associated with ciliary receptor cells and vertebrate visual pigments, though some are known to participate in neural activity of invertebrates (Randel et al., 2013; Velarde et al., 2005). Non-visual, c-type, pteropsins in crustaceans are limited to genomic data from *Daphnia pulex* (Colbourne et al., 2011), and their function in crustaceans remains uncharacterized. A second group of non-visual opsins includes the peropsins. These are distinct from pteropsins and cluster with several other groups of RGR opsins with largely unknown function; this group has tentatively been termed the Group 4 opsins (Porter et al., 2012; Sun et al., 1997). The only currently identified crustacean peropsin was identified by transcriptomic analyses of the copepod *Calanus finmarchicus* in a comprehensive opsin review, but has provided no insights as to the function or localization of this protein (Henze and Oakley, 2015). R-type opsins are found in rhabdomeric receptors - most commonly present in the visual systems of invertebrates. In particular, arthropod r-type visual opsins cluster into evolutionary groups based on their spectral absorbance characteristics and have been classified into three subgroups: long-wavelength sensitive (LWS), middle-wavelength sensitive (MWS), and short-wavelength or ultra-violet sensitive (SWS/UVS) (Porter et al., 2012). Within the stomatopod phototransduction cascade, a surprising diversity in opsin proteins has been observed in comparison to the known photoreceptor types (Cronin and Bok, 2014; Porter et al., 2013, 2009). Stomatopod species with 16 photoreceptor types, appear to express different numbers of opsin genes with *Hemisquilla californiensis* expressing at least 14 opsins, (Porter et al., 2013), while others like *Pseudosquilla ciliata* and *Neogonodactylus oerstedii* expressing as many as 33 opsins – over twice the number of photoreceptors present (Megan Porter, University of Hawaii at Mānoa, personal communication). Understanding patterns of opsin expression within the stomatopod retina may provide insights into the functionality of this large visual opsin diversity in the already numerous photoreceptor types.

As though the molecular and structural components of adult stomatopods were not perplexing enough, there is an incredible metamorphosis of the visual system during development (Cronin and Jinks, 2001; Feller et al., 2014). After a period of brooding, larvae are released into the water column where they become planktonic. The eyes at this stage are similar to that of many other crustacean

larvae: regular arrays of ommatidia forming a generally spherical eye on an eyestalk (Feller and Cronin, 2014). These paired compound eyes have pigments constrained to the very center of the eye in order for the larvae to remain as invisible as possible (Feller and Cronin, 2014). During later larval stages, the early adult retina begins to build itself on top of the larval structures (Feller et al., 2014). Early in retinal development, the adult structures remain pigment free, mainly developing new crystalline cone arrangements and accumulating dark pigments as larvae near final stages (Williams, Greenwood, & Jillett, 1985). Though the number of molts of the planktonic stomatopod larvae has yet to be determined for most species, the last-stage larvae often have a unique double-retina eye, which contains the remaining larval retina and much of the new adult retina, simultaneously (Feller et al., 2014). By the final molt to benthic juvenile, many of the larval retinal structures have degenerated or been removed (Cronin & Jinks, 2001). This newly formed adult eye is an entirely new optical system with larger photoreceptors and many new visual pigments (Cronin & Jinks, 2001). Whether transitions in the phototransduction cascade occur during development between the completed larval retina and developing adult retina remain uninvestigated, though evidence exists that the adult retina begins functioning early and in conjunction with the larval retina (Feller et al., 2014, 2013).

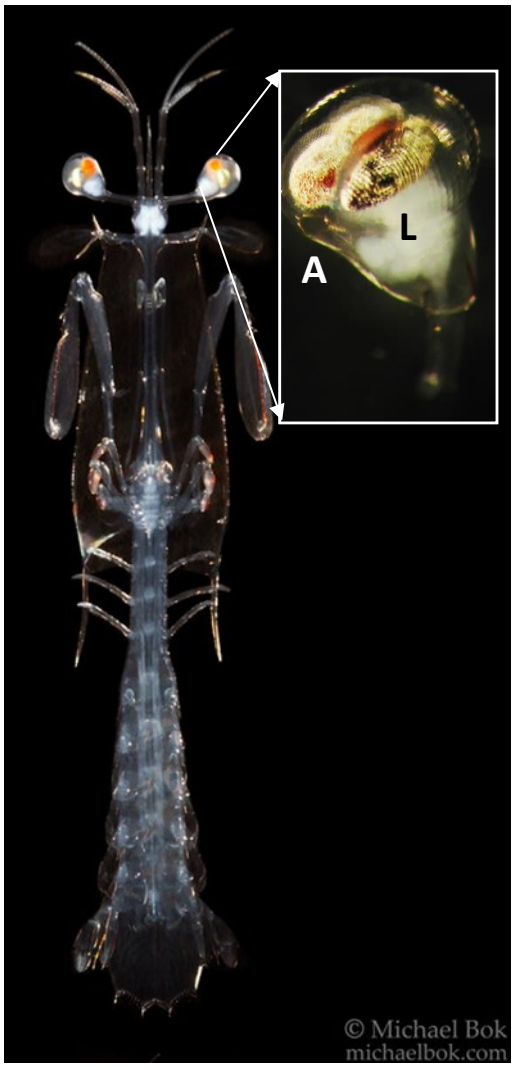

Figure 2.1 *Alima pacifica* last stage larva (photo by Michael Bok) with double retina inset distinguishing orange pigmented adult (A) and reflective larval (L) retinas (photo by Katheryn Feller).

The stomatopod, *Alima pacifica* (Squillidae, Squilloidea), has an unusually large last-stage larvae which features clearly distinguishable adult and larval retinas for dissection (Figure 2.1), presenting an excellent system to compare phototransduction in different developmental retinas within one individual. Comparing the expression of vision-related genes in the larval retina, which has begun degenerating, with the developing adult retina may provide valuable insights into opsin diversity

and expression from different developmental stages of the stomatopod. No previous molecular characterization of *Alima pacifica* phototransduction has yet occurred, and findings here may illuminate the differences in developmental photoreceptor sensitivity that has been observed in this species (Feller and Cronin, 2016). Additionally, the adult eye of *A. pacifica* has evolved a midband formed of two rows of photoreceptors, where other stomatopods have six (Porter et al., 2010). In addition to a reduced number of midband rows in this and other Squilloid species, the R8 cells in other Squillidae are reduced and lacking in microvilli (Schönenberger, 1977) or only one type of photoreceptor is present (Cronin et al., 2010). Because of this reduction in the midband rows and the photoreceptors in the adult eye, I hypothesize that *A. pacifica* will express a smaller number of opsin proteins than other stomatopod last stage larvae. The opsins identified here will provide insights into the relationships between eye development, complexity and related molecular components. Using Illumina transcriptome datasets from the eyes of last stage *A. pacifica* larvae, which were individually dissected into adult and larval retinal tissue, I have identified the expression of several known arthropod phototransduction genes. Opsin transcript expression levels were compared in larval versus adult retinal tissue and the implications of patterns present were evaluated in the broader context of crustacean visual system evolution and development.

Methods and materials:

Specimen Collection and preparation

Light trapping was used to collect last-stage *Alima pacifica* larvae off the shores of Lizard Island, Australia in April of 2013 (one individual), and again in March of 2014 (2 individuals). The eyes of each individual were dissected – pooling adult retinal tissue separately from larval retinal tissue – and immediately fixed in RNA later® (Ambion) for a total of six samples (3 larval retinas, 3 adult retinas). RNA extractions were performed using the manufacturer's protocol from a NucleoSpin® RNA XS kit (Macherey-Nagel GmbH & Co. KG, Düren, Germany) and stored at -80°C until sequencing. All samples were sequenced at Molecular Research LP (Shallowater, TX) within a month of collection. Samples from 2014 were sequenced using the Ion PGM system using the Ion 318™ Chip v2 (Life Technologies) to generate 12 and 14 million reads of varying length (for adult and larval tissue respectively). Later samples were sequenced using an Illumina MiSeq system to generate between 82 and 100 million paired end reads 150bp in length for analysis (Table 2.1).

Paired Read Transcriptome Assembly and Phylogenetically Informed Annotation

Initial read integrity of individual read sets were assessed using FastQC (v0.10.0) software, and all Illumina sequenced reads were trimmed to remove the first 9 bases and the last 5 bases to remove low quality bases, using the publically available FastXToolkit (v 0.013; http://hannonlab.cshl.edu/fastx_toolkit/) software. Ion torrent sequenced reads were also cleaned using FastXToolkit to trim the first nine bases and after 250 bases. Low quality reads were removed using FastxQuality Filter (-q 20, -p 70%) and reads below 50 bases in length were removed using FastxClipper. Reads were *de novo* assembled from Illumina Sequenced libraries on the National Center of Genome Analysis Support's (NCGAS; Indiana University, Bloomington, IN, USA) Mason Linux cluster using Trinity v2.1.1 (http://trinityrnaseq.sourceforge.net/) software to generate a total of 126,530 transcripts. Because Trinity software assembles paired end reads, Ion Torrent sequenced data was excluded from assembly and used only in later mapping (Figure 2.2). Transcripts were assessed using Phylogenetically Informed Annotation (PIA) using default parameters to identify r-type phototransduction elements (Speiser et al., 2014). Identified opsin contigs were aligned using a standard MUSCLE© algorithm (Edgar, 2004) on opsin datasets provided from Henze and Oakley (2015) and Porter et al. (2012). After initial alignment, large gaps were removed from short sequences by hand, and regional realignments were performed using a ClustalW2 algorithm (Larkin et al., 2007).

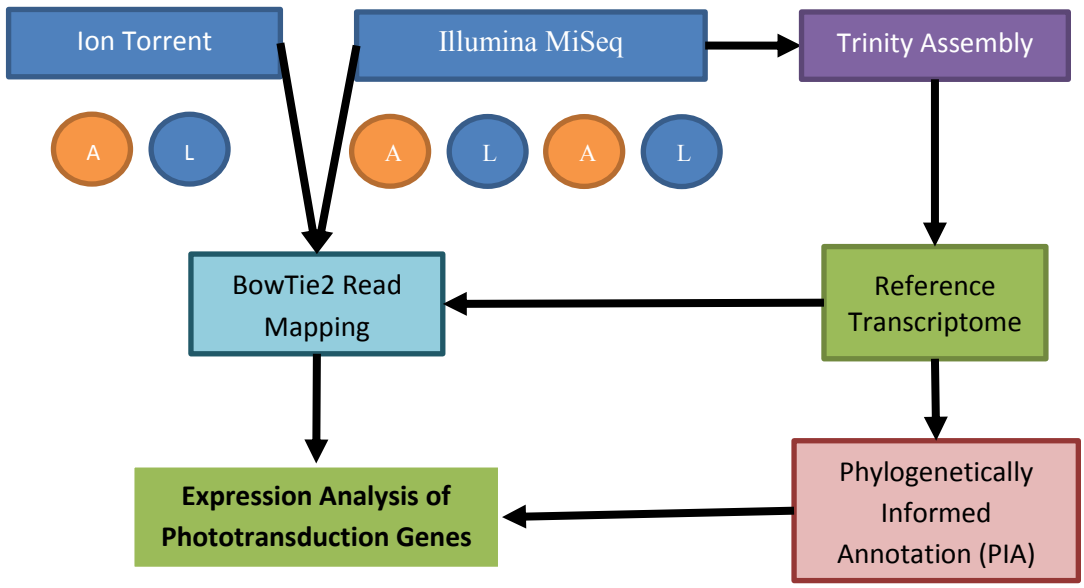

Figure 2.2 Diagram of workflow used to analyze RNA extractions from adult and larval retinal tissue.

Phylogenetic trees were reconstructed from amino acid alignments on CIPRES servers (Miller *et al.,* 2010) using RAxML (Stamatkis *et al*., 2005, 2008; Preiffer & Stamatkis, 2010) with a WAG protein model (Feller et al., 2013). A maximum likelihood phylogeny of established opsins (Henze and Oakley 2015; Porter et al. 2012) with identified *Alima* opsin contigs confirmed evolutionary placement of all PIA-identified opsins among r-type, c-type, and group 4 opsins. This phylogeny was rooted using closely related GPCRs (Porter et al., 2012). To support the suggested sensitivity of the novel SWS opsins identified in *A. pacifica,* a phylogenetic tree using known UV opsins from the insects *Apis mellifera* (NP_001011605), *Drosophila melanogaster* (AAA28856, AF184224_1), *Pieris rapae* (BAE19945, BAE19946), and the stomatopod *Neogonodactyus oerstedii* (AIF73507-9) was constructed as described above using a blue sensitive opsin from *Apis cerana* (BAH04515) to root the tree (Wakakuwa et al., 2010). Amino acid residues at positions 71 and 132 of the *Apis mellifera* UV sensitive opsin were compared across species; these residues are confirmed to participate in spectral tuning of UV opsins in invertebrates (Bellingham et al., 1997; Wakakuwa et al., 2010).

Expression Levels

The assembled *Alima* transcriptome, generated from Trinity, was used as the reference for raw read mapping of individual adult and larval tissue datasets using BowTie2 (v. 2.2.3) with default parameters to generate expression levels for all samples. Read mapping was also performed on the NCGAS Mason Linux Server (Indiana University, Bloomington, IN, USA) and RPKM was calculated as reads per kilobase of transcripts per million total reads (RPKM) (Mortazavi et al., 2008) to normalize the expression of each phototransduction gene identified by the PIA workflow by transcript length.

Opsin expression (RPKM) was averaged for all adult and larval datasets separately after a two-way ANOVA established no significant differences in transcript expression among developmental stage. Color coded heat maps grouped expression values into low (0-9 RPKM), moderate (10-999RPKM) and high (>1000RPKM) expression levels. Other phototransduction components were clustered using Ward's method and robust standardization (Mojena, 1977) was used to generate heat maps with individual tissue datasets as separate columns. Cluster patterns were described and comparisons between general larval and adult expression levels were made.

Results

Components of the phototransduction pathway mediated by r-type opsins and $G_q\alpha$ subunits were identified by the PIA workflow, including opsins, transient receptor protein (trp) channels, protein kinase C (PKC) and phospholipase C (PLC), G-protein subunits ($G\alpha_q$, $G_q\beta$, and $G\gamma$) and signal termination

proteins such as arrestins and rdgA (Appendix A1). Of the PIA genes, twelve contigs were identified as opsins. Opsin classes expressed in *A. pacifica* retinas were named by clades established in (Porter et al., 2012): visual opsins included long-wavelength sensitive (LWS) opsins, putative middle-wavelength sensitive (MWS), and ultraviolet sensitive or short wavelength sensitive (UVS/SWS), while non-visual opsins included peropsin and pteropsin genes (Figure 2.3). By conservative estimates, one opsin transcript was present in both the peropsin and pteropsins clades (Figure 2.4), and at least two visual opsins were present for each wavelength class within the retinal tissue (Figure 2.5). Of the ten visual opsins transcripts identified, half were partial transcripts: three contained the conserved DRY motif involved in G-protein binding (Franke et al., 1990), and two had both the DRY and QAKKM motifs involved in G-protein binding (König et al., 1989). The remaining five visual transcripts were considered full length and included both conserved G-protein binding regions, and the seventh transmembrane lysine chromophore binding site. Identified full length visual transcripts were a 431 residue SWS opsin (contig 1918), LWS isoforms 28205 i1 and i2 which were 342 residues in length, and two MWS transcripts with 414 and 300 residues (contig 75868 and 15021 respectively); these are marked with stars in Figure 2.5. Both UVS opsins clustered closely, and with very high support (BS = 100) with UV2 opsin from *Neogonodactylus oerstedii* (Figure 2.6). Spectral tuning sites for both UV opsins were Alanine and Phenylalanine, which are dehydroxylated when compared to residues at sites 71 (Serine) and 132 (Tyrosine) in *Pieris rapae*, indicating a hypsochromic shift (Figure 2.6, Wakakuwa et al., 2010). The non-visual opsins were full length transcripts as well, with the peropsin having 374 residues, and the pteropsin being the longest sequence with 475 residues.

Gene Expression

Several opsin isoforms were identified by Trinity, though expression patterns for these isoforms – particularly in LWS opsins, were variable (Figure 2.5). LWS opsin 28205 had three identified isoforms, but expression levels for these transcripts were only present in adult retinal tissue for the first isoform, and minimally present (RPKM<1) in larval tissue for the second and third isoforms (Figure 2.5). A single LWS opsin (62817) was highly expressed in both retinas, but much more so in larval stages. One MWS opsin (15021) was expressed similarly at low levels in both larval and adult tissue. Two isoforms of MWS opsin 49639 and a third transcript (75868) exhibited expression in both adult and larval tissue, though expression was higher in larval tissue. Two UVS opsins were expressed in both larval and adult tissue, though one UVS opsin (81924) was only expressed in one individual, and at a much lower level than the other UVS opsin present (12918). Peropsin and pteropsin were expressed at similar levels between larval and adult retinas, but peropsin was more highly expressed in general than pteropsin (Figure 2.4).

Phototransduction signaling components, while producing many isoforms from Trinity assembly, expressed multiple isoforms largely for rdgA and arrestins, and a select few isoforms for $G_q\beta$ subunits, PLC norpA, and trp channels. Two main clusters in the heat map produced a group of moderately expressed transcripts (rdgA, trp, PLC and $G_q\beta$) and highly expressed transcripts (arrestins, PKC inaC, $G_q\alpha$ and $G_q\gamma$) (Figure 2.7). One arrestin (22481) was highly expressed in both adult and larval retinas, and was significantly higher in adult retinas (Figure 2.7).

Discussion

Opsins

General opsin diversity in *Alima pacifica* was consistent with previous stomatopod findings of high opsin diversification. A total of ten opsin transcripts identified in *A. pacifica* were identified as visual r-type opsins, which is among the lower diversity observed in stomatopods. It has been observed that another squilloid, *Squilla empusa*, has fewer photoreceptors than other species , and is hypothesized to express only a single visual pigment (Cronin et al., 1993), which would suggest the recovered opsin diversity for *Alima pacifica* remains higher than would be predicted based on the physiology of Squilloid retinas. Additionally, all r-type opsins identified here were expressed at some level within either larval or adult retinal tissue, indicating these are active proteins present in the visual systems of these animals even at the early developmental stages of adult retinas and degenerative stages of larval retinas.

The presence of multiple r-type opsins in the eye of *A. pacifica* may also indicate this animal is using color vision. For color vision to occur, a minimum of two different opsins need to be expressed in at least two different types of photoreceptors of the retina (Marshall et al., 2007b; Rajkumar et al., 2010). Although the number of photoreceptors for *A.pacifica* has yet to be determined, the presence of so many r-type opsins likely indicates the presence of multiple spectral types of photoreceptors in these animals, despite the closely related species *Squilla empusa* (Cronin et al., 2010, 1993) and *Squilla mantis* (Schönenberger, 1977) having only one. In stomatopods with more complex midbands, color vision is thought to primarily occur in rows 1-4, due to the stacking of three photoreceptors in each of these ommatidia. The midbands of other Squilloids have previously been thought to most closely resemble the structure of midband rows 5 and 6, which are primarily involved in polarization and spatial vision (Porter et al., 2010). However, polarization and spatial vision can also involve multiple visual pigments (Cronin et al., 2010), with the arrangement of rhabdomere microvilli determining visual sensitivity. To further elucidate the structure and function of *A. pacifica* photoreceptors, microspectrophotometric analyses to

characterize the spectral sensitivity of photoreceptors across the retina, and *in situ* hybridization studies to identify retinal expression patterns of each transcript are crucial next steps.

While pteropsin and peropsin were expressed in both adult and larval retinas (at low and moderate levels respective to the opsins), little is known of the visual significance of these classes. Peropsin has been suggested to play a role in detecting light or monitoring photoreceptor derived compounds (Sun et al., 1997), and in invertebrates it has been localized to non-visual cells in the retina (Nagata et al., 2010). This is the second crustacean peropsin to be identified following transcriptomic analyses from *Calanus finmarchicus* (Henze and Oakley, 2015) though functional characterization of this opsin is still needed. The presence of pteropsin was surprising as, thus far, expression has been localized to invertebrate brain tissue, and is not found in the retina. Because the eyes of *A. pacifica* are on a very long stalk, it is unlikely that brain tissue was present in the multiple eyes dissected, however neuropils from the lamina are possible contaminants. The low expression levels may indicate pteropsins are present in the lamina beneath the retinas, rather than retinal tissue. The eyestalk of stomatopods has three other neutrally integrated lobes including the medulla externa, medulla interna and medulla terminalis (Prete, 2004), which may also express pteropsins, though further investigation is needed. The function of pteropsins in invertebrates is hypothesized to be related to circadian or photoperiodic behaviors (Arendt et al., 2004; Velarde et al., 2005), which may be the case in *A. pacifica* as well.

Developmental Opsin Patterns

Several opsins were clearly expressed at higher levels in larval retinas (such as MWS) compared to adult retinas. Some of this may be due to the continued development of the adult eye, which has yet to complete all visual structures. As seen by an UVS opsin (contig 12918), however, some components are capable of extremely high expression in the early stages of the adult retina development, which may indicate these photoreceptors are built or required first for the development of adult visual systems.

Three isoforms of the LWS opsin (contig 28205) were lowly expressed in adult tissue, and were hardly expressed in larval retinas. Because adult retinas are still in the process of developing, the low expression of these LWS may increase once *Alima pacifica* have reached adult stages. The single LWS opsin (contig 62817) that was expressed significantly higher in larval retinas may suggest a shift in opsin expression during development. This, coupled with all the identified MWS opsins dominantly expressed in larval retinas, provides support for this hypothesis. Previous studies of adult and larval *A. pacifica* photoreceptors have indicated that a shift in wavelength sensitivity occurs; larval retinas are more sensitive to shorter wavelengths (467nm) while adult retinas are most sensitive at longer wavelengths

(479nm) (Feller and Cronin, 2016). The dominance of MWS opsins in larval retinas, coupled with the increased number of LWS opsins expressed higher in adult retinas (Figure 2.5; Appendix A2) provide support for this suggested shift. The habitat of larval *A. pacifica*, a simple light field in the open ocean, may necessitate fewer visual requirements than the habitat of the adult stomatopod, which burrows in the shallow intertidal zone. This change in habitat would be a likely cause for any developmental shifts observed here, though more work to look at opsins expressed in completely developed adult retinas needs to be done to confirm this hypothesis.

Unexpectedly, both SWS opsins clustered more closely with other Ultraviolet Sensitive (UVS) opsins and were expressed at moderate and high levels in both adult and larval retinal tissue. One such opsin (contig 12918) was expressed at such a high level (2277 RPKM) that it almost certainly indicates the UV sensitive photoreceptors must be an early visual necessity for developing adult retinas. To find two UVS opsins is particularly puzzling, as other squilloids have very reduced R8 cells, in which UV sensitivity is not known to occur (Schönenberger, 1977). When compared to other UV sensitive opsins from the stomatopod, *N. oerstedii*, and insects (Figure 2.6), it is clear that these opsins share both known spectral tuning sites. It has been suggested that loss of hydroxyl groups, and gains of charge at residue 71 and 132 in *Pieris rapae* UV sensitive opsins results in a hypsochromic shift of λ_{max} (Wakakuwa et al., 2010). In both locations of the SWS transcripts here, a substitution of Alanine (*A. mellifera* UVop residue 71) and Phenylalanine (*A. mellifera* UVop residue 132) has occurred, indicating an accompanying blue shift is very likely (Wakakuwa et al., 2010). Additionally, both UVS opsins cluster with the UV2 opsin of *N. oerstedii* with high support (BS = 100, Figure 6), and would be likely to have a similar λ_{max} of 375nm (Bok et al., 2014). Further research as to the location of these and other opsins present should elucidate the prevalence, and spectral properties for the general diversity of opsins identified here.

Phototransduction Signaling Components

Though many phototransduction signaling components were identified from the PIA output (Appendix A1), a select few groups of these proteins were expressed in the retinas of *A. pacifica* (Figure 2.7). Clusters of low, moderate and high expression were observed, and no clear developmental differences were found, indicating larval and adult retinal tissue may be using the same visual phototransduction pathways at similar levels.

Regulatory components

The primary G_q subunits utilized by *A. pacifica* are likely similar to those of other arthropods, including *Drosophila melanogaster*, *Homarus americanus*, *Culex quinquefasciatus*. One $G_q\alpha$ subunit

(contig 14757) was expressed higher than other G_q subunits, and is most likely to be a visually involved protein. Downstream in the phototransduction cascade, transient receptor potential (trp) and trp-like (trpl) channels were moderately expressed with the trpl transcript (40045) expressing highly, likely indicating this is a primary ion channel involved in visual tasks. Likely a similar mechanism for calcium transport from the system of *Drosophila melanogaster* is occurring to depolarize cells in *A. pacifica*.

Terminating Components

Several arrestins were expressed at varying levels (moderate to high) in both adult and larval retinal tissue. One transcript for an arrestin 2 (contig 22481) was highly expressed across all tissue types, and was significantly higher in adult retinas. The same general pattern was seen in the major regulatory components of the visual system ($G_q\alpha$, trpl; Figure 2.7), which may indicate the adult visual system is ramping up activity, while larval retinas degenerate. Seven rdgA isoforms were moderately expressed in all tissues. The function of rdgA remains largely unclear; it is known to dephosphorylate active opsins, though the downstream applications of this event have yet to be fully realized. The consistent expression of rdgA in the retina of *A. pacifica,* may suggest this is an important visual protein and further work should be done to understand its importance.

Summary

The visual system of *Alima pacifica* may closely resemble that of *Drosophila melanogaster* in the phototransduction signaling components, with G_q proteins activating PLC and PKC to open trpl channels resulting in depolarization of cells. Arrestins and rdgA are likely the terminating components of this cascade. Twelve opsins were identified in *A. pacifica*; the lowest number of opsins found in a stomatopod thus far. This may be due to the reduction in the number of midband rows as compared to other stomatopod species. Non-visual peropsin and pteropsin were identified and expressed at moderate and low levels in both adult and larval retinas, though the function of these two visual pigment protein classes remains unclear. The MWS and LWS opsins identified here suggest a shift in dominant opsins between larval and adult retinas, with the suggested direction moving from shorter wavelength sensitivity in larval retinas to longer wavelength sensitivity in adult retinas. The SWS type opsins present here are unique, in that all are clustered with UV sensitive crustacean opsins where *A. pacifica* is not expected to have UV sensitive photoreceptors. To understand where the expression of each of these opsin classes is taking place, particularly for the UVS opsins, and whether the observed opsin shift is occurring, more work needs to be done.

Table 2.1 Statistics of sequencing and Trinity assembly for adult and larval retinal tissue.

	Adult Retina	Larval Retina
Measured Statistic		
Sequencing		
Sequencing Yields (Mb)	20,924	20,200
Total number of raw reads	40,167,216	38,959,957
% GC	40.71	39.69
Trinity Assembly Statistics		
Average contig length (bp)	714	
N50 contig length (bp)	1030	
Number of contigs	126,530	
N50 number of contigs	96,759	
Minimum contig length (bp)	324	
Maximum contig length (bp)	10,795	

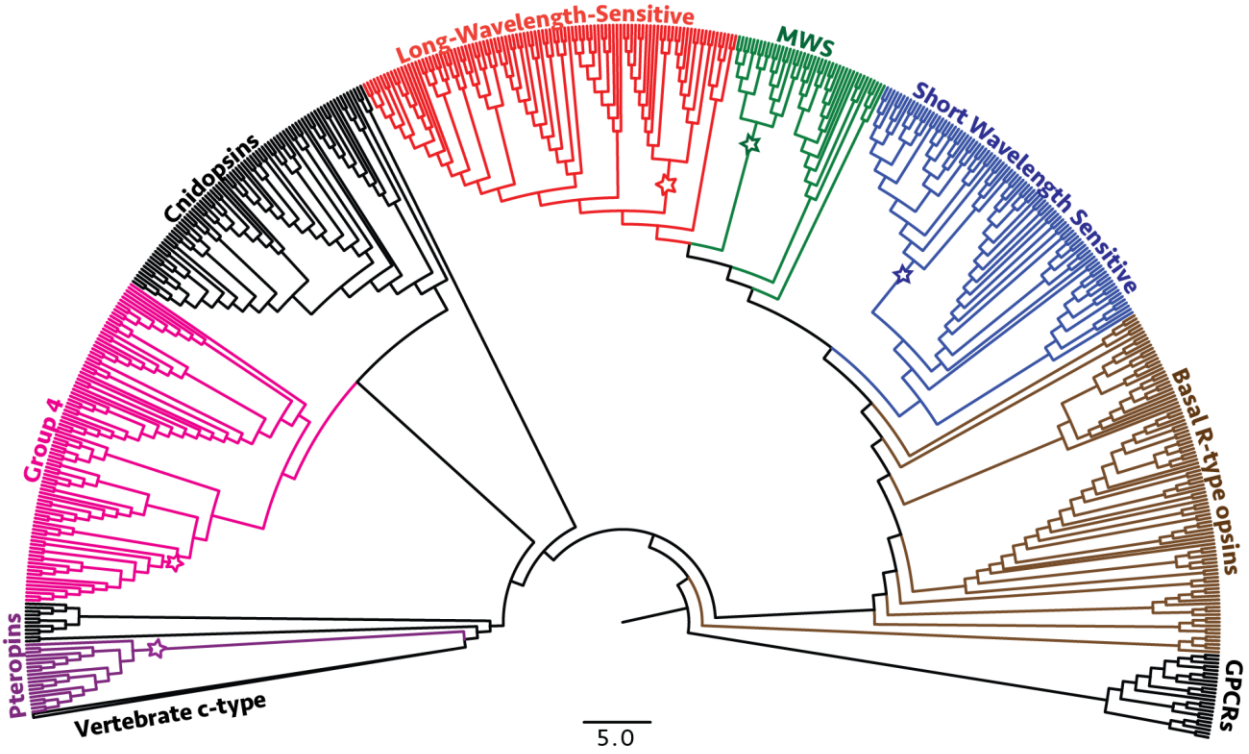

Figure 2.3 Maximum likelihood phylogeny of visual opsin proteins in arthropods, including *Alima pacifica* retinal transcriptome contigs. The tree was rooted using closely related GPCR proteins (outgroup). Clusters of opsin clades are grouped by color and named, according to (Porter et al., 2012), as Pteropsins (purple), Group 4 (pink), Cnidopsins, LWS opsins (red), MWS opsins(green), SWS/UVS opsins (blue), and basal r-type opsins (brown). The sequence diversity within the vertebrate c-type opsin clade is collapsed as a triangle. Stars indicate clades in which opsins were identified in *Alima pacifica* retinal tissue and also indicate starting nodes for zoomed in views for pteropsins and group 4 opsins (Figure 2.2) and r-type opsins (Figure 2.3).

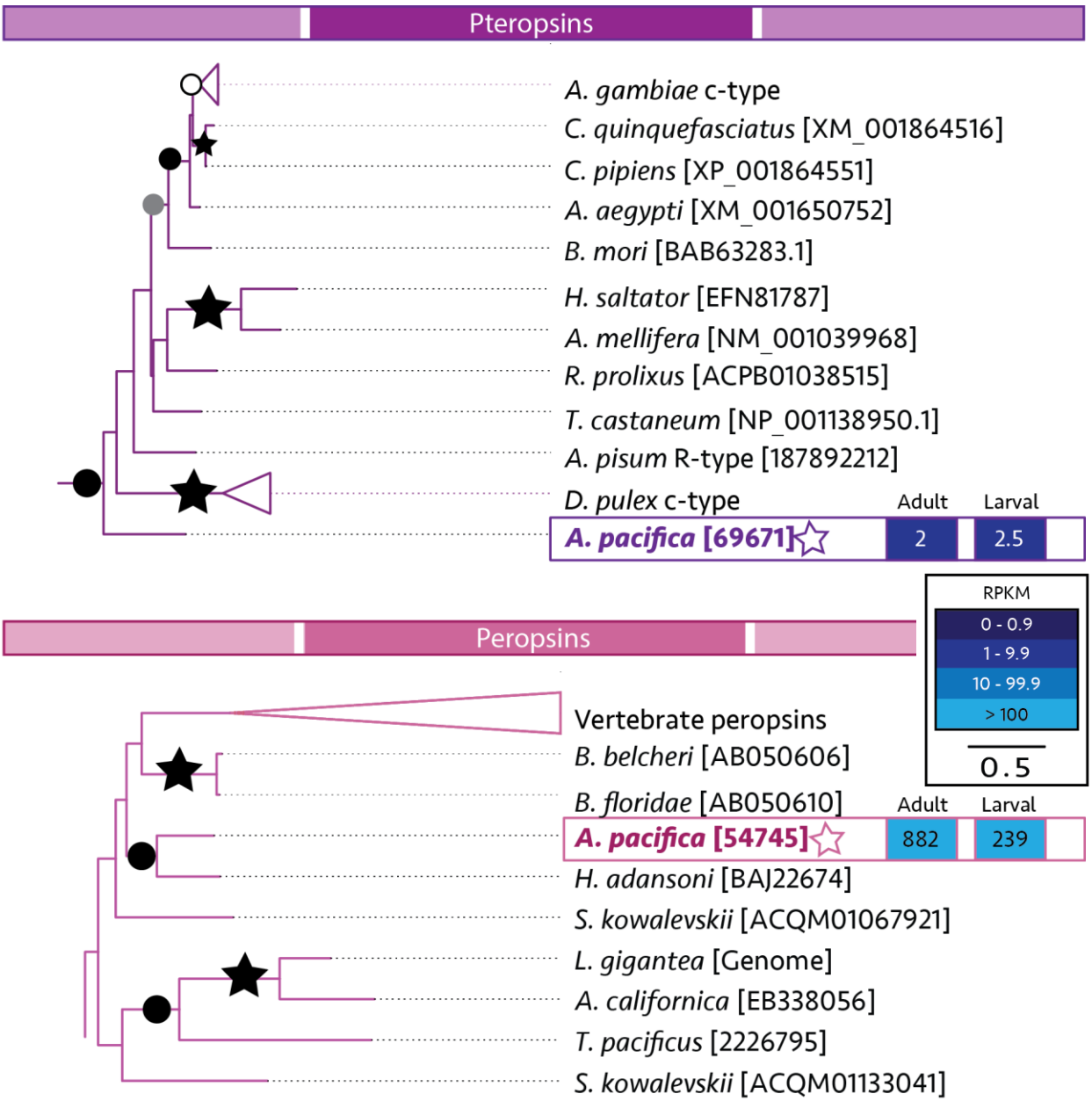

Figure 2.4 Zoomed views of maximum likelihood opsin phylogeny (Figure 2.2) for pteropsins (purple) and peropsins (pink). Bootstrap values are represented as black stars (100%), black circles (90-99%), gray circles (80-89%), and black outlined, white circles (70-79%). Individual opsins identified are highlighted with a box, and opsin expression for adults (left) and larvae (right) are represented by colored boxes to indicate relative RPKM values (low : dark blue to high : light blue). White stars next to sequence names indicate full length transcripts were identified.

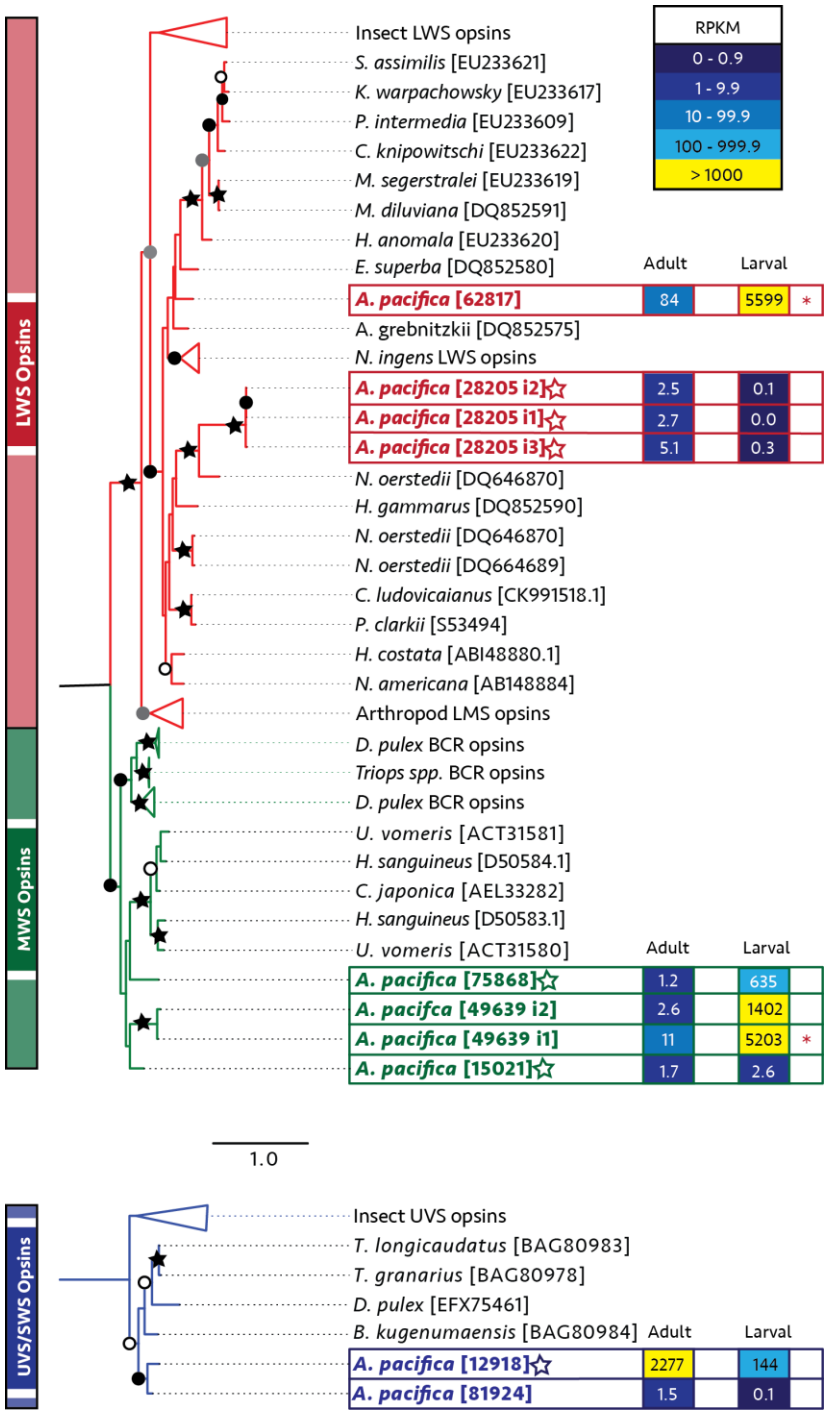

Figure 2.5 An expanded view of r-type opsin phylogeny for SWS (blue), MWS (green), and LWS (red) opsins identified in *A. pacifica*. Bootstrap values for nodes are represented by black stars (100%), black circles (90-99%), gray circles (80-89%) and white circles (70-79%). Average expression values (RPKM) of adults (left) and larvae (right) are represented next to identified transcripts in colored boxes which correspond to relative RPKM values (low, dark blue to high, yellow) of adult and larval retinal tissue. White stars next to sequence names indicate full length transcripts; asterisks after expression levels indicate significant differences between at least one adult and larval retinal pair ($P < 0.001$).

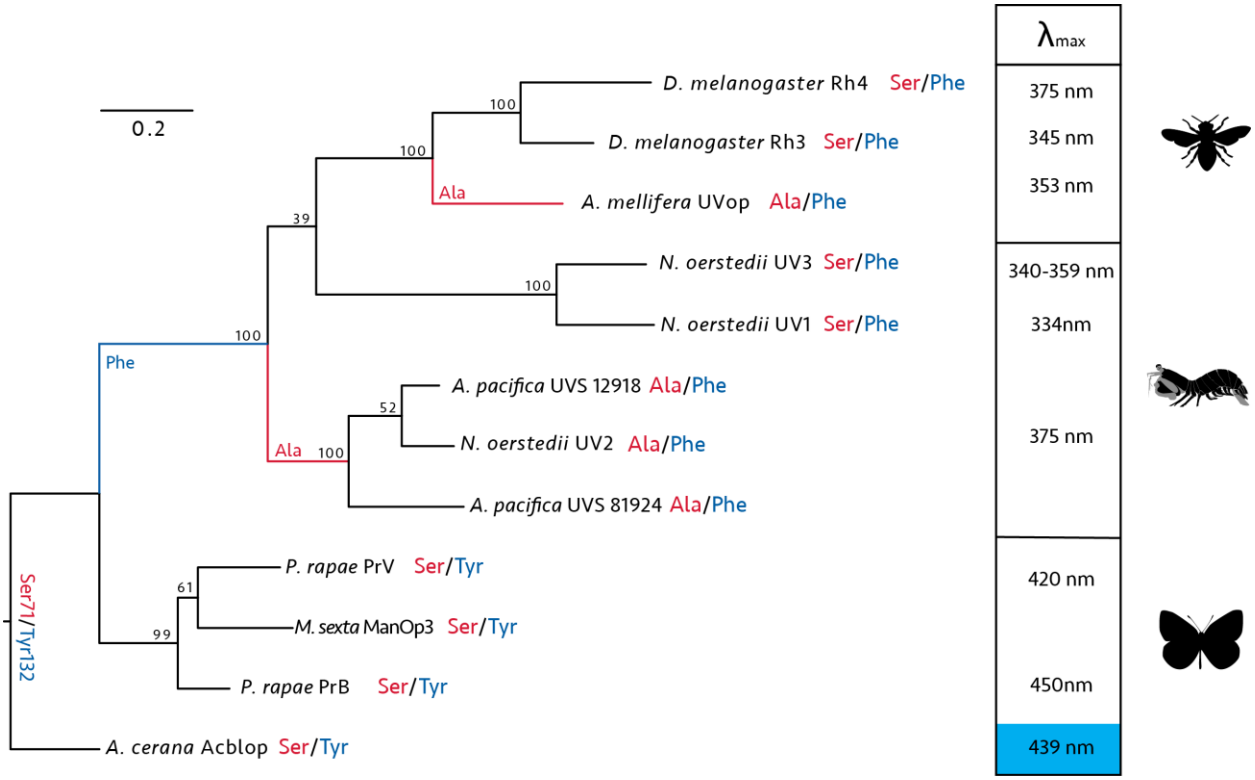

Figure 2.6 Maximum likelihood phylogeny of insect and stomatopod UV opsins, rooted using *A. cerana* blue-sensitive opsin (Acblop). Amino acid residues aligned to 71 (red) and 132 (blue) of *A. mellifera* UVop follows the name of the species and protein. Red lines indicate the substitution of alanine for serine at 71 and blue lines indicate substitutions of phenylalanine for tyrosine at 132. The spectral sensitivity (λ_{max}) of known proteins occupy the column on the right; these values were taken from literature for the insects *Drosophila melanogaster* (Feiler et al., 1992), *Pieris rapae* (Wakakuwa et al., 2010), and *Apis mellifera* (Townson et al., 1998), and for the stomatopod *Neogonodactylus oerstedii* (Bok et al., 2014).

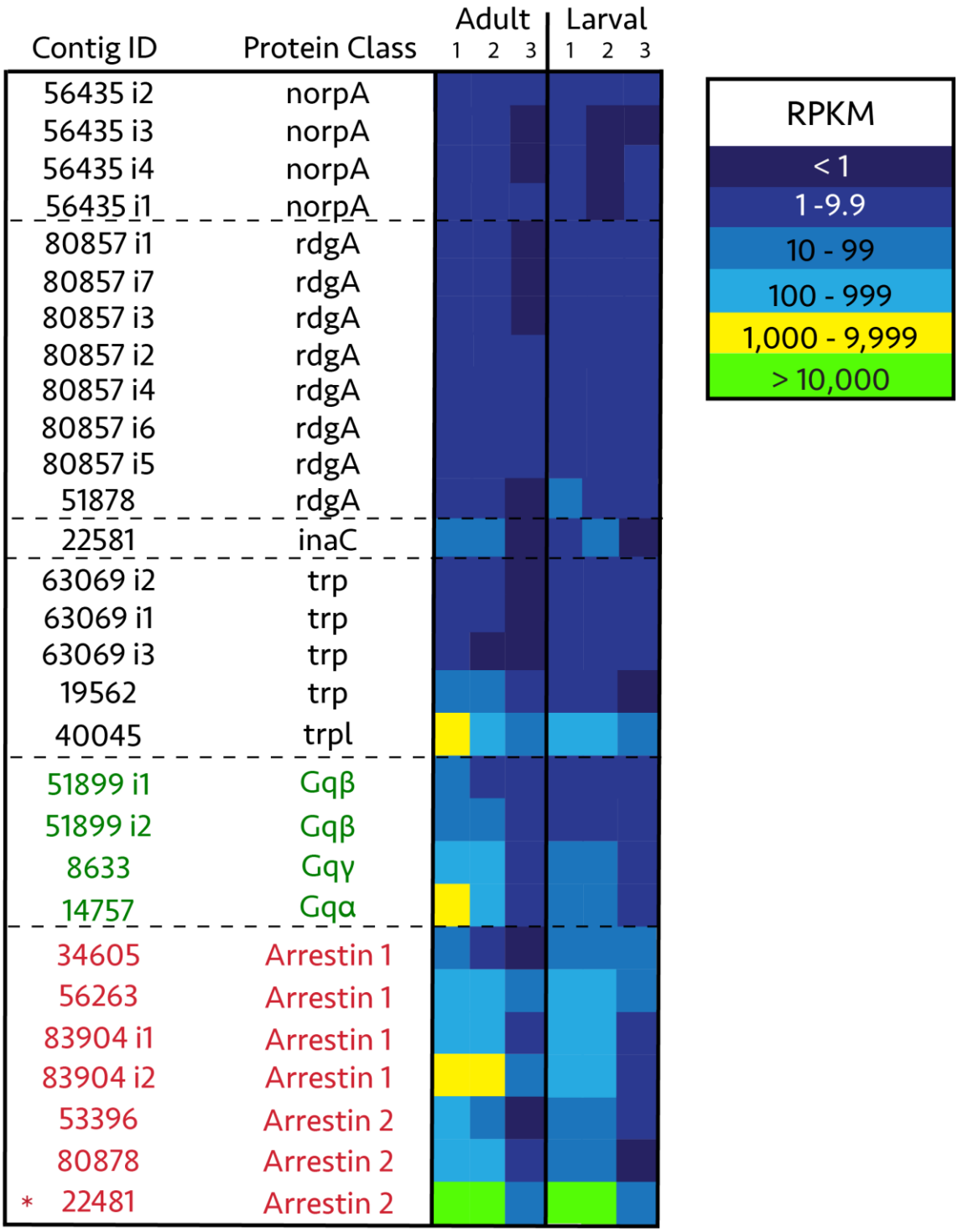

Figure 2.7 Relative expression (RPKM) heat map of phototransduction components (excluding opsins) present in *Alima pacifica* adult (left) and larval (right) retinal tissue. G-protein units are represented in green, while arrestins are represented in red lettering. Statistical significance in expression levels between at least one larval and adult retinal pair is represented by an asterisk ($P < 0.001$).

CHAPTER 3:
THE MOLECULAR CHARACTERIZATION OF PHOTOTRANSDUCTION IN THE CALANOID COPEPODS, *NEOCALANUS FLEMINGERI* AND *LABIDOCERA MADURAE*

Introduction

Crustacean visual systems are some of the most diverse of any taxa in terms of eye structure and morphology (Cronin and Porter, 2008). The structural diversity is mainly constrained to compound eye types, but some groups also have simple eyes or no eyes at all (Cronin and Porter, 2008; Elofsson, 2006; Henze and Oakley, 2015; Nilsson, 2013). While studies of the molecular aspects of vision in crustacean compound eye types have increased, fewer studies have looked at the naupliar crustacean eye types. Based on a few well studied arthropod model organisms (e.g. *Drosophila melanogaster* or *Daphnia pulex*), the general phototransduction cascade within crustacean eyes is thought to be relatively conserved, though few components of non-model crustacean visual systems have been extensively characterized (Kashiyama et al., 2009; Porter et al., 2013). To date, no studies have comprehensively looked at the molecular components involved in vision of simple eyes in copepod crustaceans, with the exception of a few visual pigments identified in *Tigriopus californicus* and *Calanus finmarchicus* (Henze and Oakley, 2015).

Visual pigments, composed of an opsin protein covalently bound to a chromophore, are sensitive to specific wavelengths of light and initiate phototransductive cascades. Opsins are an integral part of phototransduction and are the best studied molecular component of crustacean visual systems. This diverse group of proteins is specifically tuned to different wavelengths of light (Henze and Oakley, 2015; Porter et al., 2012). While the general structure of an opsin is conserved as a 7-transmembrane protein, the protein sequence itself is highly diverse among taxa and even within species (Briscoe, 2000; Kashiyama et al., 2009; Porter et al., 2012).

After photoactivation by opsins, phototransduction cascades (in most arthropods) are regulated by heterotrimeric G-proteins and transient receptor potential (trp) calcium channels (Warrant and Nilsson, 2006). The $G_q\alpha$ subunit of the heterotrimeric G-protein binds to activated opsins and initiates the cellular cascade by disassociating from the other subunits ($G_q\beta$ and $G_q\gamma$) to interact with downstream effectors, such as phospholipase C (PLC), protein kinase C (PKC), or adenylate cyclase (Warrant and Nilsson, 2006). Activation of these proteins results in the opening of transient receptor potential (trp) calcium channels, which cause depolarization of the cell. The signaling cascade is terminated by arrestins, which bind to active opsins and halt activity.

Whether similar levels of molecular complexity exist for visual systems in simple crustacean eyes has yet to be established. The copepods are a particularly interesting group because they have simple eyes and exist in habitats with low visual structure. The open ocean habitat has a simple light field, yet many complex visual behaviors have been observed in copepods. Vertical migration and phototaxis have been extensively characterized in these small creatures (Cohen and Forward, 2002; Conover et al., 1988; Machida and Tsuda, 2010; Mackas and Louttit, 1988; Waggett and Buskey, 2007) and there is some evidence that copepods may respond to bioluminescent warning cues (Buskey and Swift, 1985), wavelengths corresponding to twilight (Cohen and Forward, 2002), and predator shadows (Waggett and Buskey, 2007). In the North Pacific, for example, aggregations of calanid copepods, dominated primarily by *Neocalanus*, have been found to collect at the surface waters during rapid changes in light intensities (Conover et al., 1988; Mackas and Louttit, 1988; Tsuda et al., 1999). The documented visual tasks required by these animals have prompted research into the structure and function of the copepod eyes.

While there are difficulties in studying the eyes of these miniscule organisms, several studies have structurally characterized the eyes of at least 24 species of copepods (Elofsson, 2006). The structure of copepod visual systems are relatively well conserved, typically consisting of simple frontal eyes with wide visual fields (Nilsson, 2013; Warrant and Nilsson, 2006). These naupliar eyes are quite exceptional among the crustaceans in their lack of ommatidial units and lenses, and the difference in photoreceptor organization (Elofsson, 2006). Three distinct pigment cups with complex innervation (Elofsson, 2006; Land, 1988) form a tri-partite eye, in which two lateral cups and the ventral cup have joined together (Elofsson, 2006). Most copepods, without modified naupliar eyes, have ten sensory cells in each lateral cup, and nine sensory cells in their ventral cup (Elofsson, 2006; Warrant and Nilsson, 2006). These eyes are much less complex when compared to the compound eye structure of many other crustacean frontal eyes (Elofsson, 2006), and therefore provide a unique look into a “simpler” crustacean visual system.

Though these eyes have fewer structural components than compound eyes, they are no less a visual enigma. Within the subclass Copepoda, there is frequently transformation of the frontal eyes (Elofsson, 2006; Land, 1988); members of the pontellids are often sexually dimorphic, with males having much larger eyes than females, suggesting a visual need for mate recognition (Ohtsuka and Huys, 2001; Warrant and Nilsson, 2006). The tri-partite eye of the pontellid, *Labidocera madurae,* has separated into three distinct eyes (Figure 1) – one ventral, and two dorsal (Ohtsuka and Huys, 2001). The dorsal eyes of this species are complex, having a large, spherical lens overlying an eye-cup with eight receptors.

Additionally, the two eye-cups are joined together in this species and connected to muscles and elastic strands, an adaptation which allows the eyecup scanning movement (Land, 1988). Though both sexes have mobile eyes, only males are observed to exhibit scanning behavior systematically (Warrant and Nilsson, 2006).

While the adult eye of copepods has been well characterized structurally, the reorganization of the larval eye to the adult eye is currently not well understood. Copepods undergo three developmental stages: nauplius, copepodite and adult. Nauplii represent the first six stages of a copepods life cycle; these stages often have rudimentary appendages primarily used for feeding. After several molts, the copepodite stage is reached, which resembles an early, adult copepod. As copepodites molt from first (C1) to last (C5) stage, the number of legs increase and the cephalothorax lengthens. It is during the late copepodite stages that sexual dimorphism begins to differentiate morphologically (Peterson, 2001). As early as the first nauplius stage, a tri-partite eye has been observed (Lacalli, 2009) though the transition (or lack thereof) to an adult eye and the mechanism required for such a transition remains unclear.

To date, very few published molecular studies of copepod visual systems have been conducted, and none have looked at the development of the eye from a molecular perspective. Here, we will use transcriptomic approaches to characterize the expression of potential phototransduction components in the visual system of *Neocalanus flemingeri* late copepodites to molecularly characterize a "typical" copepod eye with a simple frontal eye structure. *Neocalanus flemingeri* is an ecologically significant species due to its prevalence in the subarctic Pacific Ocean where they, along with other large grazer species, are vital links between primary production and predators of these regions (Kobari and Ikeda, 2001). To further understand the evolution and development of copepod visual systems, transcriptomic analyses of late copepodite stages and adult female *Labidocera madurae* were done to provide insights into the transformed frontal eyes of copepods. These analyses will add to our understanding of the mechanism behind copepod vision by identifying transcripts for proteins which initiate (opsin visual pigments), transduce (G-proteins), and terminate (arrestins) the phototransduction cascade.

Materials and Methods

Copepod Collection

Female and copepodite stages of *Labidocera madurae* (Pontellidae, Calanoida), were collected using light traps from He'eia harbor in Kaneohe bay, located in Windward Oahu, Hawai'i. Individuals were transported alive back to the Pacific Biosciences Research Center (PBRC) at the University of

Hawai'i at Mānoa and developmental stages were identified. Copepods were grouped by developmental stage: at least 5 adult females were pooled per sample and at least 15 late copepodites were pooled as a sample with three replicate samples per developmental stage for whole body RNA extraction.

Late copepodite *Neocalanus flemingeri* (Calanidae, Calanoida) copepods were collected via plankton tows from the Prince William Sound in the Gulf of Alaska (May 2015). Zooplankton were collected using a Carvet Net towed vertically through the upper 50m of the water column and CV stage *N. flemingeri* were live sorted. Three replicate samples from each tow, containing two CV stage *N. flemingeri* per sample, resulted in a total of 12 samples. Copepodite pairs were fixed in RNAlater® solution and stored at -20°C until transported to PBRC, where samples were stored at -80°C until total RNA extraction could occur.

Transcriptomes

For each species, total RNA was extracted from pooled specimens and sample concentration and quality were checked via a 2100 Bioanalyzer system (Agilent Technologies, 2016). RNA quality was evaluated via comparison of 18S and 28S peaks according to Lenz et al. (2014). Multiplexed gene library sequencing was performed at the University of Georgia Genomic Facility (August, 2015) using an Illumina® NextSeq Flow Cell. NextSeq 500/550 kits for whole transcriptomes (Illumina® Inc., 2016) were used to prepare total RNA for sequencing, using the mid output kit for *N. flemingeri* and high output kit for *L. madurae*, to generate paired end reads up to 150 bp in length. Libraries generated 211 million paired-end raw reads for *N. flemingeri* and 528 million paired-end raw reads for *L. madurae*.

Raw reads were trimmed using the publically available FastQToolkit (v.2.0: Illumina BaseSpace Labs) after quality assessment in FastQC (v1.0.0, Babraham Bioinformatics). The first 9 bases were trimmed from all reads, Illumina adapters were removed, and reads with phred scores lower than 30 were removed from the *L. madurae* datasets, while phred scores of lower than 20 were removed from *N. flemingeri*. Reads less than 50bp in length were removed from raw read datasets using FastQToolkit. Cleaned reads for each species were *de novo* assembled using Trinity software (version 2.0.6) on the National Center of Genome Analysis Support's (NCGAS; Indiana University, Bloomington, IN, USA) Mason Linux cluster. Assembly statistics were generated using Trinity's statistic function and a custom perl script.

Phylogenetically Informed Annotation

Generated assemblies were uploaded to Galaxy servers at the University of California Santa Barbara (UCSB) and analyzed using the Phylogenetically Informed Annotation Workflow (PIA) as described by Speiser et al. (2014). This method fits translated nucleotide contigs into pre-established maximum likelihood trees of a metazoan Light Interaction Toolkit (LIT) for rapid analysis of predicted visual proteins. Although 144 genes are included in the LIT, proteins specifically initiating (opsin visual pigments), transducing (G-proteins), regulating (trp) and terminating (arrestins) the phototransduction cascade were the main focus. PIA-predicted opsin contigs were extracted and amino acid sequences were compared for percent similarity. Isoforms predicted by Trinity having 100% similarity in amino acid sequence were removed from further analysis. Identified opsins were then aligned using MUSCLE algorithms (Edgar, 2004) to a larger opsin data set taken from Porter et al. (2012). After initial alignment, large gaps were removed from short sequences by hand, and regional realignments were performed using ClustalW2 algorithms (Larkin et al., 2007).

Phylogenetic trees were reconstructed from amino acid alignments on CIPRES servers (Miller *et al., 2010*) using RAxML (Stamatkis *et al*., 2005, 2008; Preiffer & Stamatkis, 2010) with a WAG protein model (Henze and Oakley, 2015). An initial phylogeny of established opsins from Porter et al. (2012) with identified copepod opsin contigs confirmed evolutionary placement of all PIA-identified opsins among the R-type and C-type opsins. This phylogeny was rooted using closely related GPCRs (Porter et al., 2012). Copepod opsin sequences identified as r-type were realigned to an additional opsin dataset from Henze and Oakley (2015) and Porter et al. (2012) to provide more information between phylogenetic relationships. Short-wavelength sensitive (SWS) opsins taken from Porter et al. (2012) were used to root this phylogeny. Other copepod opsin sequences clustering with invertebrate c-type opsins were realigned with vertebrate c-type opsins, arthropod c-type opsins (pteropsins) and cnidarian opsins from Porter et al. (2012) using cnidarian opsins as an outgroup.

Gene Expression Analysis

Raw reads datasets were mapped back to their respective species transcriptome (*L. madurae* or *N. flemingeri*) using Bowtie2 (version 2.2.3) on Mason Linux cluster (NCGAS, Indiana University, Bloomington, IU, USA) as described by (Lenz et al., 2014; Roncalli et al., 2015). Relative expression, of all mapped transcripts was normalized by length, calculating reads per kilobase of transcript per million mapped reads (RPKM) for each library (Mortazavi et al., 2008). Here, expression levels of 72 phototransduction genes identified from PIA were looked at.

Heat maps were generated in JMP statistical software (SAS, 2016) to color code RPKM values into groups of expression levels for PIA identified visual transcripts of each sample. For *N. flemingeri,* low expression was established as all values below 1RPKM, moderate expression as 1-9.9RPKM, and high as greater than 10RPKM. The relative expression levels were higher in *L. madurae*, therefore moderate expression ranged between 1 and 99.9RPKM, while high expression was considered as values above 100RPKM. Individual expression values were grouped by protein identification and resulting expression patterns were observed and described. A two-way ANOVA, using sample and transcript ID as factors, was done to look for significant differences in expression values.

Results

Sequencing and assembly of copepod transcripts were distinct between species, generating a total of 256,438 unique transcripts (contigs) for *N. flemingeri* and 211,002 contigs for *L. madurae* (Table 3.1). Several unique transcripts for putative phototransduction genes were identified in both copepods including visual pigments (opsin), $G_q\alpha$ proteins, trp channels, and arrestins (Table 3.2). Of the genes identified in both species, similar numbers were present, with the exception of opsins and trp channels, which were more numerous in *L. madurae*.

Visual Pigments

A total of 14 opsin transcripts were identified, clustering within two major phylogenetic clades of known arthropod opsins: a putative middle-wavelength sensitive (MWS) clade and an arthropod ciliary type opsin clade, known as pteropsins (Figure 3.2). By conservative estimates, the number of contigs represents three MWS opsins in *N. flemingeri*, compared to six in *L. madurae*, and three pteropsins in *L. madurae* compared to two present in *N. flemengeri* (Table 3.2).

Identified *N. flemingeri* and *L. madurae* r-type opsins formed a moderately-supported clade (Bootstrap (BS) > 70, Figure 3.3), clustering with other publically available copepod opsins also considered to be middle-wavelength sensitive (Porter et al., 2012). Identified MWS opsins formed three well-supported (BS > 80), monophyletic clades for the species *Calanus finmarchicus, Labidocera madurae,* and *Neocalanus flemingeri*. *L. madurae* isoforms (87318 i1, i2) create a sister group to the Harpacticoid copepod, *Tigriopus californicus* [ADZ45237], though additional data will likely reveal a different relationship due to the low bootstrap value. Two *Neocalanus flemingeri* opsins (26285 and 19649) form a sister group to other calanoid copepod opsins, including *Labidocera* and *Calanus*, and the harpacticoid, *Tigriopus*.

Contigs clustering with other arthropod pteropsins formed a unique copepod clade with moderate support (BS > 80). Pteropsin transcripts from *Neocalanus* formed a distinct clade, separate from *Labidocera* with high support (BS > 90).

General Phototransduction Components

Several regulatory components, including G_q protein subunits (α, γ, and β), phospholipase C (PLC) and calcium gated transient receptor potential (trp) channels were identified from the PIA workflow. In general, numbers of phototransduction gene contigs were similar between species, with the exception of trp channels, which had a higher number of isoforms in *L. madurae*, but more unique transcripts in *N. flemingeri* (Table 3.2). Proteins that play a role in inactivating opsin, such as arrestins and rdgA were also identified in PIA and present in similar contig numbers (Table 3.2).

Gene Expression

In general, more PIA identified transcripts were expressed in *N. flemingeri* than in *L. madurae*. Clusters of high, moderate, and low expression were found in both individuals, though phototransduction components within these clusters were not necessarily similar. It is clear from the expression analysis of *L. madurae* that both adults and copepodites express at least four unique opsins (Figure 3.5) at differing levels. Several transcripts defined unique clusters dependent upon developmental stage (in *L. madurae*, Figure 3.6).

Labidocera madurae

BowTie expression levels revealed several unique patterns between developmental stages of *L. madurae* (Figure 3.6). High expression was observed in MWS opsin contig 87318 in both adults and copepodites, though each copepodite sample expressed this opsin significantly higher than any adult sample ($P < 0.0001$). This pattern of higher copepodite and lower adult expression was also observed arrestin 2 (52048 i3) and $G_q\gamma$ (26758), though was not significant. Generally low expression was observed in several other contigs, including identified trp, the PLC, norpA, and pteropsin transcripts. Of the major proteins involved in the phototransduction cascade, one contig for an initiating MWS opsin (ID 87318), a $G_q\alpha$ subunit (ID 62931), a trp channel (ID 35939), and an arrestin (ID 54755 i3) were expressed higher than other transcripts in these protein classes.

Neocalanus flemingeri

Most putative visual proteins were lowly expressed (< 1 RPKM), particularly in groups such as the G-protein subunits and trp calcium ion channels (Figure 3.6). A group of $G_q\gamma$ subunits were the only transcripts highly expressed (>10 RPKM) in most of the samples. Putative visual opsins had low

expression for most identified transcripts, though many of the pteropsins displayed moderate expression in more than one sample. A single $G_q\alpha$ subunit (ID 4539) was moderately expressed in all samples, compared to low expression for the other transcripts in this protein class. Arrestins expressed either lowly or moderately across all samples and did not appear to have a dominant transcript for the group.

Discussion

This study used transcriptomics to document the presence of major components known to be active in photoreceptor signal transduction for two species of copepod: *N. flemingeri* and *L. madurae*. Based on the phylogenetic associations of many annotated components, these copepods have the potential to utilize a Gq-mediated phototransduction pathway similar in structure to that of *D. melanogaster*. All 13 components of phototransduction from the PIA workflow were found within both copepod species (Table 3.2), though more focus will be given here to visual pigments, Gq-alpha subunits, trp channels, and arrestins.

Opsins

More opsin contigs, as compared to all other putative phototransduction components, were identified in both species of copepod. Opsin transcripts identified belonged solely to a putative MWS class and the little studied clade of arthropod c-type opsins, henceforth referred to as pteropsins. The phylogenetic relationships of the MWS opsins resulted in a separated copepod opsin lineage, with species specific groups occurring within the clade. With more data, the level of similarity among copepod species should be further evaluated to confirm whether patterns present here are reflective of true opsin diversity. When looking at the phylogenetic placement of the pteropsins, it was found that the copepods had a distinct lineage, forming a sister group to those of *D. pulex* and other arthropod species (BS>70%, Figure 3.1).

Representatives of the MWS class recovered here were estimated as 8 transcripts for *L. madurae* and four transcripts from *N. flemingeri*. This prevalence in MWS opsins is not entirely unexpected as other copepod species have been found to be positively phototactic when exposed to blue-green light (wavelengths between 420 and 580nm) and much less responsive to wavelengths outside this range (Cohen and Forward, 2002). Middle wavelength sensitivity of other crustacean opsins occurs optimally at 460 and 480nm (Henze and Oakley, 2015), which falls within the range of blue-green light. Previous research has identified eight distinct photoreceptive cells in the eye of *L. madurae* (Land, 1988) - matching the number of MWS opsin transcripts identified here. By all accounts, the diversity of

opsin transcripts identified here were more than expected for measured sensitivity – a pattern that is being observed in many other crustacean visual systems (Kitamoto et al., 1998; Oakley and Huber, 2004; Porter et al., 2009; Sakamoto et al., 1996). While the absence of opsin transcripts from other opsin wavelength sensitivity clades may be due to a number of methodological biases (ie. time of collection, RNA extraction or cDNA construction, and sequencing efficiencies), there may be true differences reflected in the opsins found in these two species. Additionally, the absence of a particular opsin class does not necessitate absence from the genome or even from expression in general for the reasons outlined above. Estimates of transcript number represented in the transcriptome of each species can still be useful in providing a baseline of gene expression for future studies.

The differences in the number of expressed opsin transcripts may also have been due to the multiple developmental stages present in *L. madurae* samples. To understand the difference in these expression patterns, read mapping was done to look for differences in opsin transcript expression levels among *L. madurae* stages. While one MWS opsin was highly expressed in both adults and copepodites, this opsin was significantly more expressed in copepodite stages than in adult stages – indicating that developmental stage likely influences the diversity of opsins present. As such, the increased number of unique opsin transcripts in *L. madurae* may have been due to the presence of adult samples which were lacking in *N. flemingeri*.

The transformed frontal eyes of *L. madurae* cannot be excluded as factors to opsin diversity in this species, however, as the adults did express all identified opsin contigs to some degree. It has been suggested that the adult eye plays a role in mate recognition and prey capture for these, often brightly colored, copepods while other calanids rely more heavily on chemical signals for these functions (Land, 1988; Ohtsuka & Huys, 2001). It is also noteworthy that pontellids have developed refractive lenses overlying the ocelli of the nauplius eye which are not present in the general set up of the simple frontal eye (Land, 1988). It is clear this species is visually oriented, and the higher opsin diversity observed here coincides with this notion. Future studies observing opsin diversity in adult male and female *L. madurae* may be pertinent as this organism is known to be sexually dimorphic, with males having much larger eyes and using the scanning motion of these eyes more than females (Land, 1988).

The visual opsins were not as moderately expressed as the pteropsins in *N. flemingeri*, suggesting that a secondary phototransduction cascade separated from the visual system of these animals is required. Because *N. flemingeri* has simpler eyes, it may be that more pteropsins are required

to initiate phototransduction cascades that regulate the light-driven behaviors displayed by these animals. Fewer non-visual opsin contigs were identified in *L. madurae* and only one was expressed at low levels, which lends support to this hypothesis. Pteropsin is known to be expressed in the brains of most arthropods, rather than in the eyes (Eriksson et al., 2013; Velarde et al., 2005); as such, it is not surprising to see a low expression level present here, due to the limited innervation a copepod eye exhibits. To date, all arthropods not expressing pteropsin in the eye have compound eyes (Eriksson et al., 2013; Velarde et al., 2005), thus pteropsin expression in the eye of these animals cannot be ruled out. Other invertebrates, such as onychophorans have exhibited pteropsin expression in the eye (Eriksson et al., 2013), which could indicate eye type plays a role in the location of expression.

Phototransduction Signaling Components

Several putative phototransduction proteins exhibited varying levels of expression in each copepod species. One of the highest expressed transcripts in *L. madurae* adults and copepodites was a trp channel (35939). Other trp channels were expressed at much lower levels, including a trpγ transcript, and were similarly expressed in adults and copepodites. *N. flemingeri* expressed consistently low levels of trp and trpγ, though many more isoforms were expressed. Uniquely, no trp-like (trpl) transcripts were identified in either species, though this is a common, visually involved, calcium channel in model organisms such as *Drosophila melanogaster* (Hardie and Minke, 1992; Niemeyer et al., 1996). In *D. melanogaster*, trpγ has been observed as a subunit which preferentially interacts with trpl. Though the absence of trpl channels in these findings does not necessitate absence from the transcriptome of these species; factors illustrated previously (time of collection, RNA extraction, cDNA construction, and sequencing efficiencies) may again be involved in transcript presence. Further analysis of light-sensitive cation channels in these species should provide more insight as to the function of trpγ and elucidate the presence or absence of trpl channels.

G_q proteins in the phototransduction cascade act as heterotrimers, generally with the three subunits: α, β, and γ. Each subunit was identified in both copepods here. In *L. madurae*, a single, G_qα subunit was moderately expressed in both copepodites and adults – though slightly higher in adults. Similarly, a G_qα transcript (4539) was highly expressed in all adult *N. flemingeri*. Two types of visual G_qβ subunits were identified (Gβ2 and Gβ 13F) with expression levels of Gβ2 being higher in copepodites, while expression of Gβ 13F was higher in adult females. This pattern may indicate a developmental shift in Gβ subunits from Gβ2 in copepodites to Gβ 13F in adults. Only G_qβ2 was identified in *N. flemingeri*, and all transcripts exhibited low expression levels. A Gγ subunit was also expressed moderately in *L.*

madurae adult and copepodite samples, though higher in copepodites, which could be another indication of a developmental shift. All $G_q\gamma$ transcripts were very highly expressed in *N. flemingeri* from all locations. Because G-proteins are commonly used in several molecular pathways, it is difficult to conclusively state that these trends are present in visual pathways, though subunits here have been established as visual proteins for many arthropods.

Two visual PLCs exhibited moderate expression levels in *L. madurae*: norpA, one of the first identified visual PLCs (Pearn et al., 1996), and inaC. A striking pattern in these PLCs was the dichotomy of expression levels: adults largely exhibited inaC at moderate expression levels, but did not exhibit the same diversity in norpA expression as copepodites. This too may indicate a developmental shift from norpA in copepodites to inaC in adults, though naupliar stages should be studied to further elucidate any potential trend. Adult *N. flemingeri* expressed high levels of inaC (45387) but relatively low levels of norpA. While it cannot be ascertained here whether a similar developmental shift from norpA to inaC may be occurring, it is of interest to note. Future studies on late stage copepodite, and even naupliar stages of *N. flemingeri* may elucidate these findings.

Arrestins and rdgA

An interesting trend in visual expression of the phototransduction cascade terminating proteins, the arrestins, was noteworthy. Two identified arrestins (Arrestin 1 - 54755 i2 and Arrestin 2 - 52048 i3) in *L. madurae* were expressed at low or moderate levels in adult females, but moderately and highly in copepodites. The expression of arrestins in *N. flemingeri* was similarly interesting in that both displayed low expression levels. The relative expression of all arrestins was similar to that of the opsins present, indicating these terminating proteins are likely to be involved in vision.

Another protein known to dephosphorylate activated opsins, rdgA, was observed in several different “isoforms”. One such contig (i2) was expressed moderately in *L. madurae* adult females and copepodites, and both other isoforms (i1 and i3) were expressed higher in copepodites, though still exhibiting only moderate expression. In *N. flemingeri*, moderate expression of one rdgA transcript (61252) was observed, while low expression of other rdgAs was seen. The moderate expression of rdgA is unique, because in *Drosophila melanogaster*, this protein is known to mediate norpA signaling (Suzuki et al., 2003) – which was lowly expressed in both species here. Due to the low levels of expression observed in opsin transcripts in *Neocalanus*, it is also likely that rdgA is not solely involved in vision of these animals.

Summary

The characterization of the phototransduction cascade for a transformed copepod eye has revealed seven opsins identified as MWS (three in *N. flemingeri* and four in *L. madurae*), five non-visual pteropsins (three in *N. flemingeri* and two in *L. madurae*), changes in developmental gene expression, and the potential of functional isoforms. Adult copepods with "typical" eyes exhibited less diversity in $G_q\beta$ subunits, though nearly all other putative phototransduction signaling components were present and expressed in similar patterns. The major pattern differences between *L. madurae* and *N.* flemingeri was the single MWS opsin found in *L. madurae* which was highly expressed in adults, and significantly higher in juveniles, while no opsins were highly expressed in *N. flemingeri*. This difference could be due to the increased complexity of the *Labidocera* eye structure, or the difference in visual system usage of these species. Further functional studies should test the hypotheses that these components are responsible for visual transduction in copepods, as tissue extractions were not retina-specific. While methodological biases and lack of retinal specific transcriptomes may have influenced the results observed here, identified opsins and patterns are likely to reflect true opsin diversity and developmental biology of these unique crustaceans. Though more work needs to be done to elucidate crustacean visual systems to the same extent of vertebrate visual systems, the work done here has produced many new findings for the field of arthropod vision.

Table 3.1 Statistics for the sequencing and transcript assembly of copepod transcriptomes using Trinity Software.

	Labidocera madurae	*Neocalanus flemingeri*
Measured Statistic		
Sequencing		
Sequencing Yields (Mb)	89,510	37,950
Total number of raw reads	528,000,341	211,083,698
% GC	40.77	43.06
Trinity Assembly Statistics		
Average contig length (bp)	872.14	583.4
N50 contig length (bp)	1184	556
Number of contigs	211002	243570
N50 number of contigs	37470	66083
Minimum contig length (bp)	301	301
Maximum contig length (bp)	23,836	12,166

Table 3.2 Expression of *L. madurae* and *N. flemingeri* genes involved in the rhabdomeric phototransduction cascade. For each component of phototransduction, the annotated contig number, number of isoforms and closest landmark sequence generated from other arthropod phototransduction genes are listed*.

	Neocalanus flemingeri			***Labidocera madurae***		
Protein Class	**contig ID**	**Isoform**	**Landmark Sequence**	**contig ID**	**Isoform**	**Landmark Sequence**
Arrestins	553	3	Arr1 [P15372]	54755		Arr1 [P15372]
	40523	2	Arr2 [P19107]	52048	2	Arr2 [P19107]
G-protein subunits	2540	5	G_qβ2 *C.quin* [XP 0018631]	66944		G_qβ2 *C.quin* [XP 0018631]
	60472		Gnαq *H.am* [P91950]	88752		Gq β 13F [P26308]
	4539		Gnαq *H.am* [P91950]	11513		Gq β 13F [P26308]
	35010		Gnαq *H.am* [P91950]	62931		Gnαq *H.am* [P91950]
	25807	5	Gq γ 30A [Q9NFZ3]	26758		Gq γ 30A [Q9NFZ3]
				41923		Gq γ 30A [Q9NFZ3]
				73762		Gq γ 30A [Q9NFZ3]
GPRKs	6158	4	Gprk1 [P32865]	9279		Gprk1 [P32865]
	36904	2	Gprk2 [P32866]	33686		Gprk2 [P32866]
	36904		Gprk2 [P32866]			
MWS Opsins	19649		Rh1 [P06002]	32108		Rh1 [P06002]
	26285	2	Rh1 [P06002]	34776		Rh1 [P06002]
	39142	2	Rh1 [P06002]	70491		Rh1 [P06002]
				87318		Rh1 [P06002]
PLC	21175	2	norpA [P13217]	19718		norpA [P13217]
	35282	2	norpA [P13217]	32637		norpA [P13217]
				60695		norpA [P13217]
PKC	45387		inaC [P13677]	50543		inaC [P13677]
C-type Opsin	44234		Pteropsin *A.mel* [NP 001035057]	43030		Pteropsin *A.mel* [NP 001035057]
	7335	3	Pteropsin *A.mel* [NP 001035057]	83724		Pteropsin *A. mel* [NP 001035057]
	19520		Pteropsin *A.mel* [NP 001035057]			
Phosphatase	8922		rdgA [Q09103]			
	20721	4	rdgA *A.mel* [XP 396522]	43707		rdgA *A.mel* [XP 396522]
	61252	4	rdgA *A.mel* [XP 396522]	54742	3	rdgA *A.mel* [XP 396522]
	21820		rdgB [P43125]	73647		rdgB [P43125]
Transient receptor potential channels	55550		trp [P19334]	10982		trp [P19334]
	57506		trp [P19334]	35939		trp [P19334]
	55901		trp [P19334]			
	13403		trp gamma [Q9VJJ7]	33102		trpgamma [Q9VJJ7]
	34962		trp gamma [Q9VJJ7]			
	43684		trp gamma [Q9VJJ7]			

*all unlabeled accession numbers are from *Drosophila melanogaster*.

A.mel = Apis mellifera, C. quin = Culex quinquefasciatus, H. am = Homarus americanus

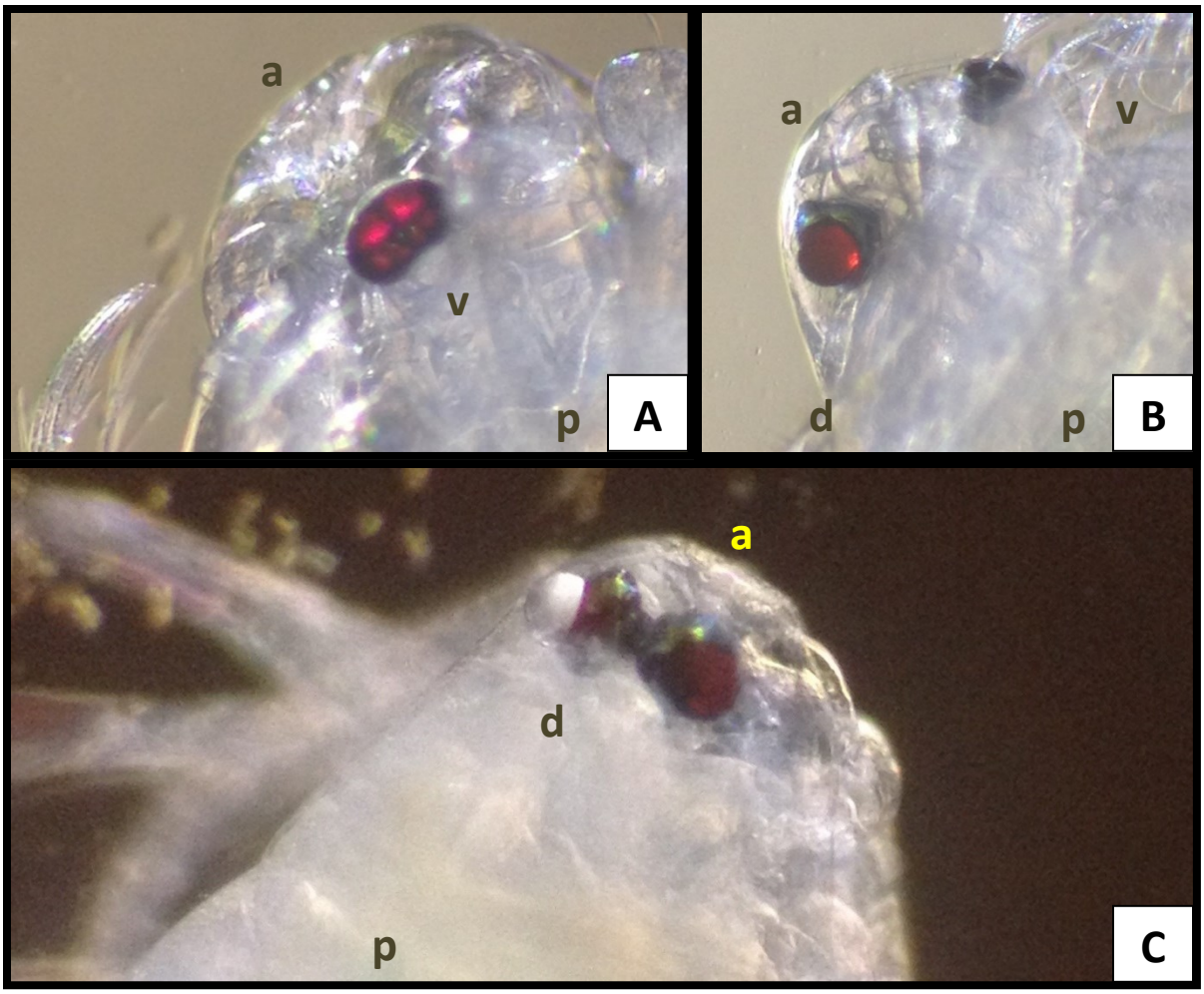

Figure 3.1 Microscopic (40x) view of adult *Labidocera madurae* (A) ventral eye (B) lateral view of one dorsal and the ventral eye (C) dorsal view of two dorsal eyes with reflective pigments. Anterior (a), posterior (p), dorsal (d) and ventral (v) of the animal are indicated alphabetically.

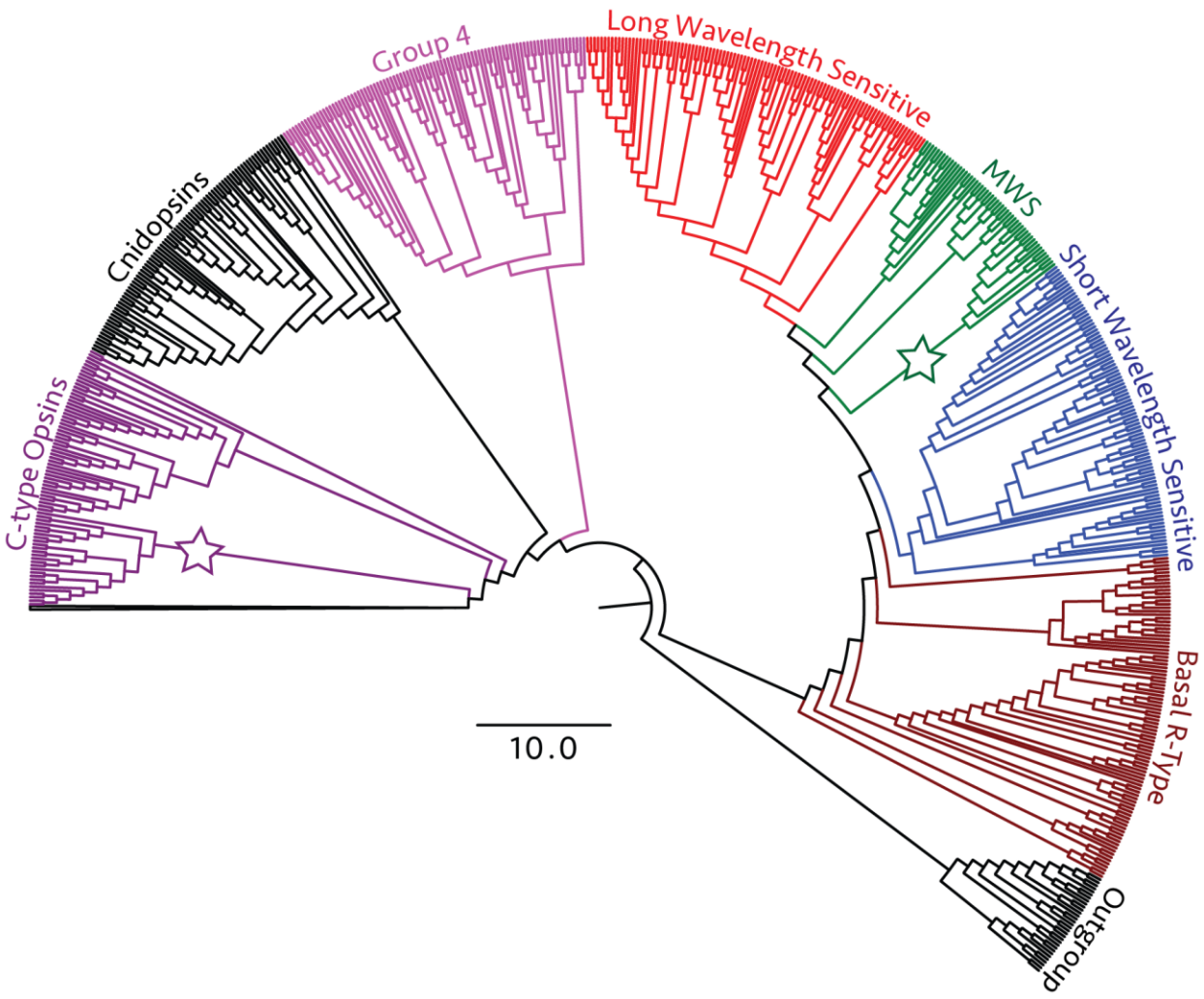

Figure 3.2 Maximum-likelihood phylogeny of metazoan opsin proteins rooted using closely related GPCRs as described in (Porter et al., 2012). Opsin clades containing identified copepod contigs are represented by a star symbol.

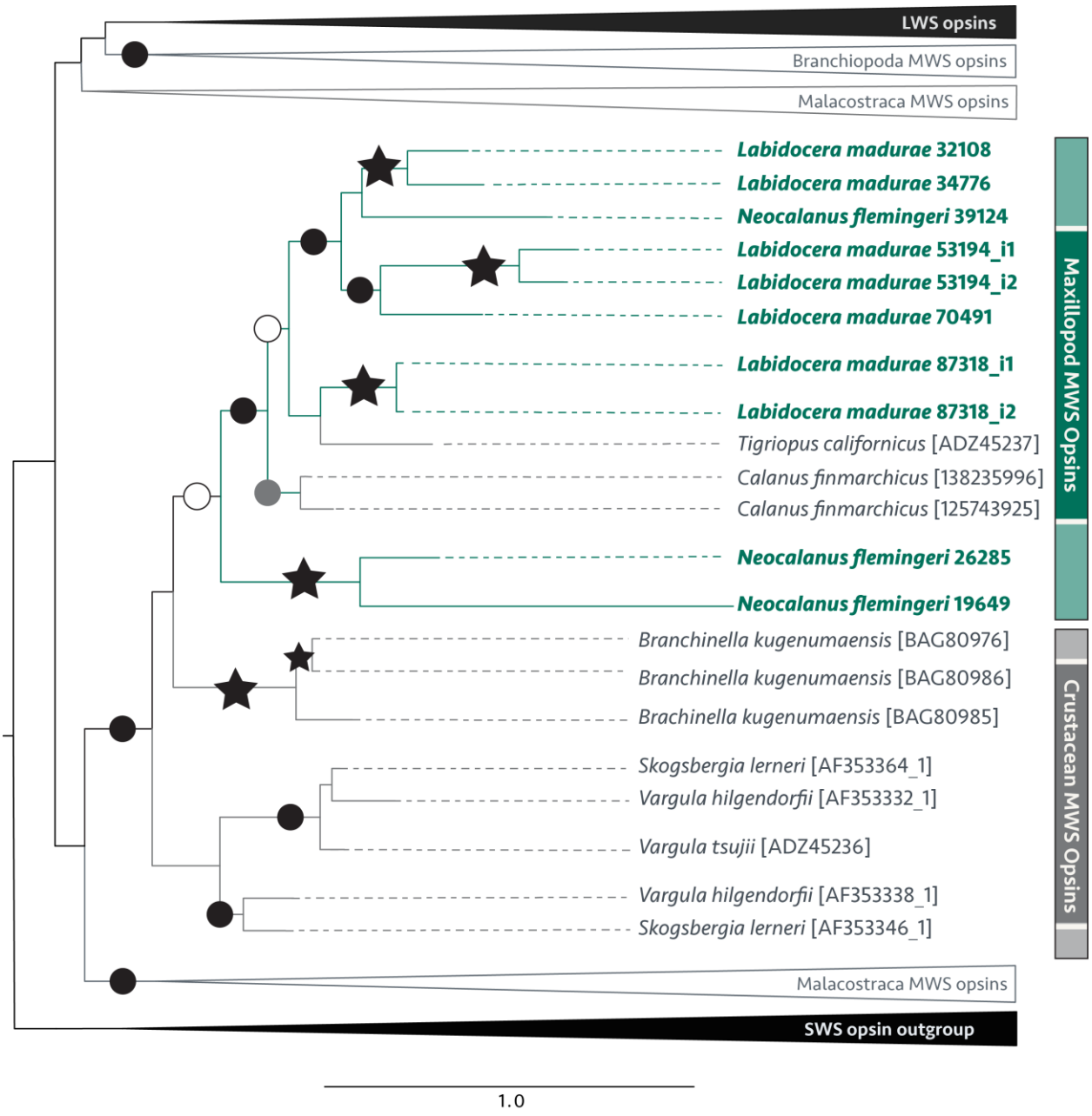

Figure 3.3 PIA-Identified visual pigments clustering with other middle-wavelength sensitive visual opsin proteins in arthropods in a new phylogeny using added MWS opsins from (Henze and Oakley, 2015). This maximum-likelihood phylogeny of arthropod R-type opsins includes *N. flemingeri* and *L. madurae* transcriptome contigs (in green). The tree was rooted using arthropod short-wavelength-sensitive (SWS) opsins from (Porter et al., 2012). Arthropod long-wavelength-sensitive (LWS) opsin diversity is collapsed and represented as a triangle. Other identified middle-wavelength-sensitive (MWS) opsins from arthropods are represented as collapsed clades with the names of arthropod classes present. Bootstrap values are represented on branches by symbols: white circles = 70-79% support, gray circles = 80-89%, black circles = 90-99%, and black stars = 100% support.

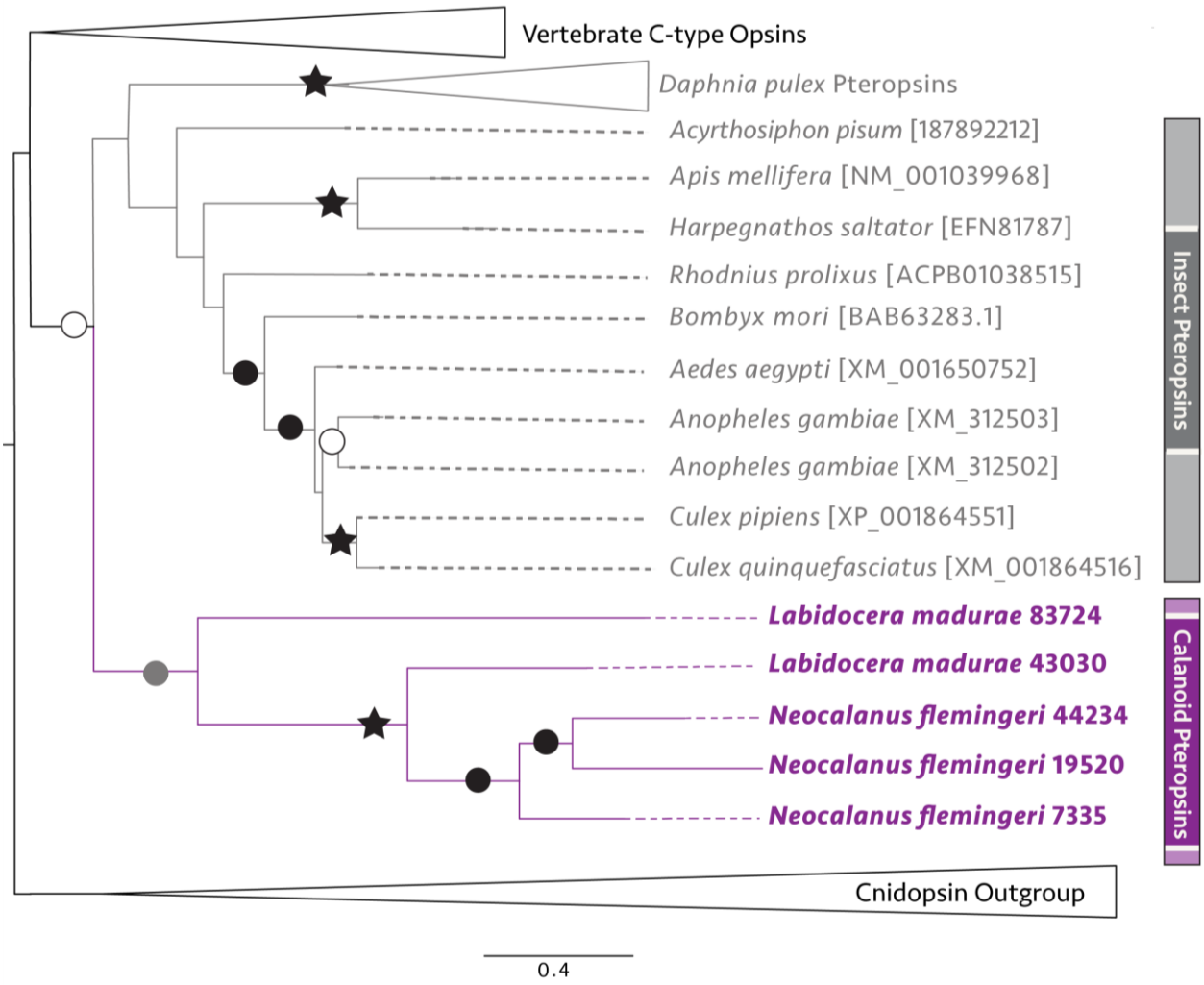

Figure 3.4 Maximum-likelihood phylogeny of non-visual opsins proteins in arthropods, including *N. flemingeri* and *L. madurae* transcriptome contigs. The tree was rooted using known visual opsins from cnidarians (cnidopsins) with vertebrate c-type opsins grouped as a triangle to represent sequence diversity within the clade Bootstrap values are represented on branches by symbol: white circles = 70-79% support, gray circles = 80-89%, black circles = 90-99%, and black stars = 100% support.

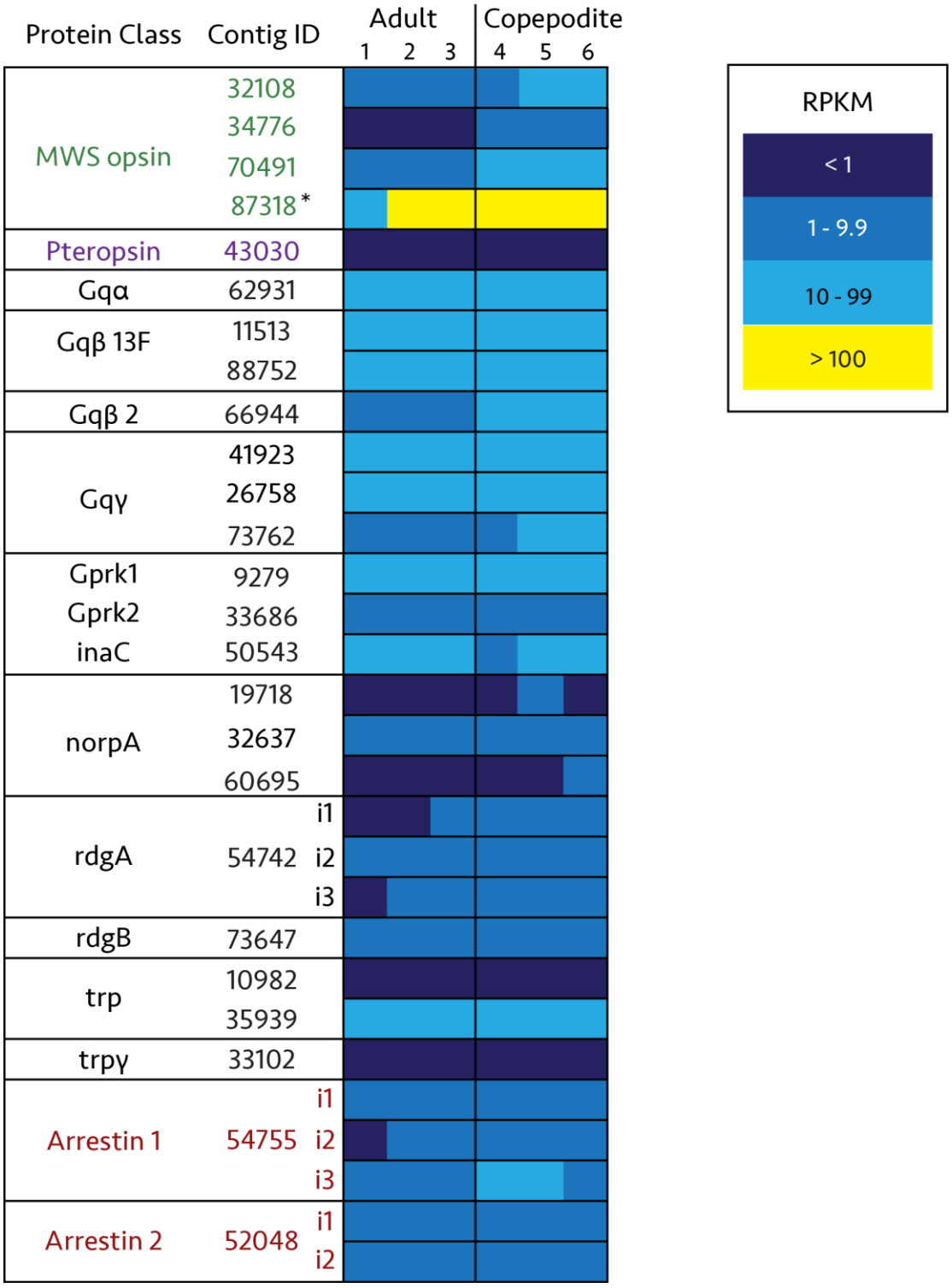

Figure 3.5 Heat map of gene expression (RPKM) for *Labidocera madurae* adult female (1-3) and copepodite (4-6) samples. Protein families identified from the PIA workflow identify mapped transcripts for each row. Signal initiating visual opsin text is green, while phototransduction terminating text is red. Values which are significantly different, from a two-way ANOVA, in at least one adult and copepodite sample ($P<0.001$) are marked with an asterisk (*).

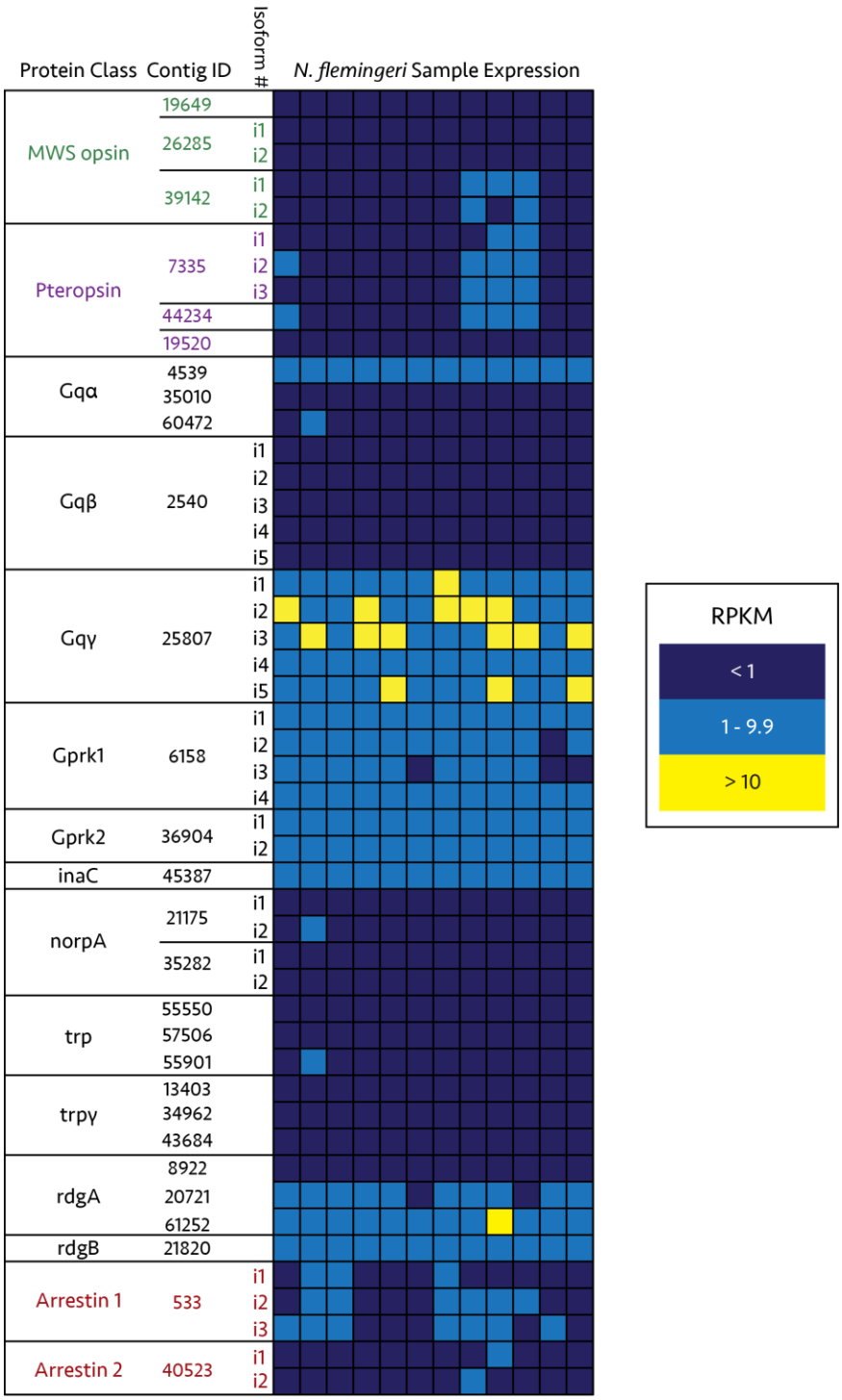

Figure 3.6 Phototransduction transcript expression (RPKM) in *N. flemingeri* across the Gulf of Alaska. Replicate samples are individual columns. Protein families identify mapped transcripts for each row. Signal initiating visual opsin text is green, and mapped pteropsins are in purple, while phototransduction terminating arrestin text is red.

Chapter 4:
Adding to the knowledge of Crustacean opsin evolution for two unusual eye types: a synthesis of the stomatopod *Alima pacifica* and the copepods *Neocalanus flemingeri* and *Labidocera madurae* visual systems

Between the bizarre naupliar eye of the copepod and the highly complex, multi-lobed apposition eye of the stomatopod, it is clear that crustaceans have a complex history of eye evolution. This research has identified 14 opsins between the two copepod species, and 12 opsins in *A. pacifica* alone. There are clear differences in the phototransduction initiating components of the visual systems of these species, though in general the rest of the cascade remains molecularly similar to that of other crustaceans. It must be remembered that all data obtained from the copepods was extracted from whole bodies, and proteins identified may not be specific to the eyes or even to the visual system of these animals.

Opsins

As was anticipated for crustaceans with less complex eyes, less visual opsin diversity existed in the copepods than the stomatopods (Figure 4.1). Only putative middle wavelength sensitive (MWS) opsins were identified in the copepods, though the number of opsins was higher in the copepod with the transformed eye (seven in *L. madurae*, three in *N. flemingeri*). Looking at the more complex eye anatomy in *A. pacifica*, four MWS opsins were identified, as well as four LWS and two UVS visual opsins, totaling to ten visual opsin transcripts. A clear pattern of increased opsin diversity was observed as eye complexity increased, though the functional relevance of this diversity remains undiscovered.
Both groups also contained pteropsins, which are thought to play a role in light sensing for circadian systems (Passamaneck et al., 2011; Randel et al., 2013; Velarde et al., 2005). Oddly, three pteropsin transcripts were expressed in *N. flemingeri* samples, while both organisms with more complex eyes expressed fewer. The reverse of the visual opsin pattern was observed as the complexity of the eye increased: more non-visual opsins were observed in organisms with simpler eyes. This may be indicative of crustaceans with reduced eyes relying on a pteropsin initiated phototransduction pathway in addition to the visual system present in the simple eye to coordinate visual behaviors. Functional studies, including *in-situ* hybridization may clarify the expression of the pteropsins in these species and elucidate the findings revealed here.

A non-visual peropsin was also identified and expressed in the both the larval and adult retinas of *A. pacifica*. There is evidence that the copepod *Calanus finmarchicus* expresses a peropsin (Henze and

Oakley, 2015), suggesting a need to look more closely into *L. madurae* and *N. flemingeri* non-visual opsins.

When phylogenetically compared using opsins from Porter et al., (2012), the lineage of the MWS opsins becomes more clear (Figure 4.1). It has been suggested that a previous arthropod ancestor had a visual system with four visual opsins progenitors, which have since diverged into the clades present today; tentatively the arthropod ancestor visual system contained one LWS opsin, two MWS opsins, and one SWS/UVS opsin (Henze and Oakley, 2015; Porter et al., 2009). The findings here are very similar, with the arthropod r-type, visual opsins forming a LWS clade, a SWS clade, and two putative MWS clades (Figure 4.1).

The visual opsins identified in the copepods here are among the first found in any copepods, with only two others having been published, one for *Calanus finmarchicus* and one from *Tigriopus californicus* (Henze and Oakley, 2015). The visual opsins for the stomatopod, *A. pacifica* had the lowest diversity thus far seen in a stomatopod and were phylogenetically compared with opsins from other stomatopod species to evaluate their evolutionary history (Figure 4.2). As previously described by Porter et al. (2009), seven LWS groups (A-F) were observed, with two of these groups containing opsins from *A. pacifica* (E and F). Group F shows signs of diverging clades with the addition of *A. pacifica* sequences, though more stomatopod visual systems need to be evaluated to fully grasp the history of the LWS opsins. The MWS and SWS opsins both diverged into two main clades, as observed for arthropods by Henze and Oakley (2015). The sequences of *A. pacifica* clustered within one clade for each expected sensitivity (MWS1 and SWSb). While some sequences identified from *A. pacifica* clustered with other members of the superfamily Squilloidea, most of them clustered near members of Gonodactyloidea. There are few published sequences for members of Squilloidea, however, and further analysis of these species may result in different relationships.

Similar developmental patterns of opsin expression were observed for MWS opsins, qith one gene having significantly higher expression levels in copepod and stomatopod larvae relative to the adults. This may be an indication of a developmental shift in photoreceptor sensitivity and diversity occurring in both *A. pacifica* and *L. madurae*. Support for developmental shifts in photoreceptor sensitivity has been found in *A. pacifica* with larval retinas being more sensitive to shorter wavelengths than adults (Feller and Cronin, 2016). It is expected that these shifts in sensitivity may be influenced by the habitats of the larval stages in comparison to the adults. *A. pacifica* larvae are largely pelagic, and settle to the benthos as adults (Feller et al., 2013); this shift in habitat likely comes with a shift in visual tasks and light exposure. Similarly, early stages of *L. madurae* are thought to inhabit deeper zones of the

water column than the adults which reside in the neuston; this shift in habitat may also influence the light exposure of the animal. Adult *Labidocera* are also known to exhibit complex visual behaviors such as mate recognition (Land, 1988). While habitat may influence the expression of opsins in copepods, it is also likely that adult visual behaviors play a role in determining photoreceptor sensitivity.

Putative Visual Signal Transducing Components

In general, components of phototransduction, including G-proteins, transient receptor potential (trp) channels, and arrestins were identified in both copepods and the stomatopod and likely resemble the visual system of *Drosophila melanogaster.*

The $G_q\alpha$ subunits are thought to be the most conserved in visual systems due to their specific interactions with opsin proteins. A maximum likelihood tree generated from known visual $G_q\alpha$ subunits of several invertebrate taxa (Figure 4.3) indicate that several $G_q\alpha$ subunits may indeed be linked to visual systems for both copepods. Interestingly, a clade of crustacean $G_q\alpha$ subunits was created, and nearly all $G_q\alpha$ subunits identified fall within this clade of other visual proteins. Only one *Neocalanus* contig (35010) was placed outside of the visual $G_q\alpha$ subunits and is not likely to be a Gq protein. Oddly, only one putative visual $G_q\alpha$ subunit was identified in *L. madurae*; this is unusual because $G_q\alpha$ subunits are involved in other signaling pathways as well. It is probable that sampling methods (ie. collection time, specimen condition, and other methodological biases) resulted in lower $G_q\alpha$ subunit diversity than actually exists within these species.

The putative trp channels identified revealed interesting expression patterns for both organisms with the more complex eyes (*L. madurae* and *A. pacifica*). In general, the expression of trp channels in *N. flemingeri* was low, though six unique contigs were present. *L. madurae* expressed only three trp transcripts and one was highly expressed in both adult and copepodite samples. Several trp channels were moderately expressed in *A. pacifica* as well, and a one trp-like (trpl) transcript was dominantly expressed in adult and larval retinas which may indicate this is a primary visual protein. The major difference in the trp transcripts expressed was that of the secondary trp channel; in the copepods, only the secondary trpγ was present, while in *A. pacifica* the secondary trpl channel has more contigs (Figure 4.4). Trpγ is thought to act as a subunit to trpl in *D. melanogaster*, so the division of these two proteins between species seems unique. Phylogenetic placement of all trp transcripts resulted in two trp channel clades for *A. pacifica* and one copepod clade with high support (BS = 94, Figure 4). While samples are based on limited taxa, due largely to the lack of characterization of visual trp proteins, placement of the trpγ channel in copepods were of interest. One transcript from *A. pacifica* did cluster closely with trpγ, but this contig was expressed at low levels in retinal tissue of *A. pacifica*. Because the stomatopod contig

evolved separately from the copepod trpγ clade but clustered with other visual trpγ proteins, all contigs identified as trpγ in copepods may not serve as visually active channels. To provide more evidence for these findings, it is vital that future research be done to investigate more closely the calcium channels which are present in crustacean visual systems.

Arrestins

Similar to the trp channels mentioned previously, arrestins were expressed at low levels in *N. flemingeri* and expressed moderate to high in both *L. madurae* and *A. pacifica*. The levels of nearly all proteins in *Neocalanus* were expressed at low levels and many more isoforms of each transcript were present, which may have been a characteristic of the sample set obtained. A maximum likelihood phylogeny of arrestins and landmark sequences from PIA (Speiser et al., 2014) resulted in species specific clades for both arrestins 1 and 2 (Figure 4.5). The arrestins of copepods delineated prior to the visual clade of arrestin 1, while those of *A. pacifica* result in a sister clade to *D. melanogaster* arrestin 1. The same pattern can be seen with arrestin 2, which may indicate the arrestins of the copepods are more basal than those of *A. pacifica*.

Summary

The molecular components of the visual system in crustaceans are remarkably well conserved despite the diversity of eye types present in this group. The general composition of the phototransduction cascade in the copepods with naupliar eyes is similar to that of the stomatopod, *A. pacifica,* all of which resemble that of *D. melanogaster*. Some developmental patterns also appear to be conserved between these taxa, with signs of developmental shifts of the dominant visual opsin. The non-visual pteropsins identified were most numerous in the least developed eyes and may be indicative of a reliance on a secondary light-sensing system in *N. flemingeri*. There is evidence that other copepods, such as *Calanus finmarchicus* also exhibit a non-visual peropsin (Henze and Oakley, 2015), which may not have been identified by the sampling methods used here. While much knowledge has been gained on the visual systems of the copepods *L. madurae* and *N. flemingeri* and the stomatopod *A. pacifica*, it is clear that much more work in understanding the complex history behind the evolution of the visual system in crustaceans needs to be done.

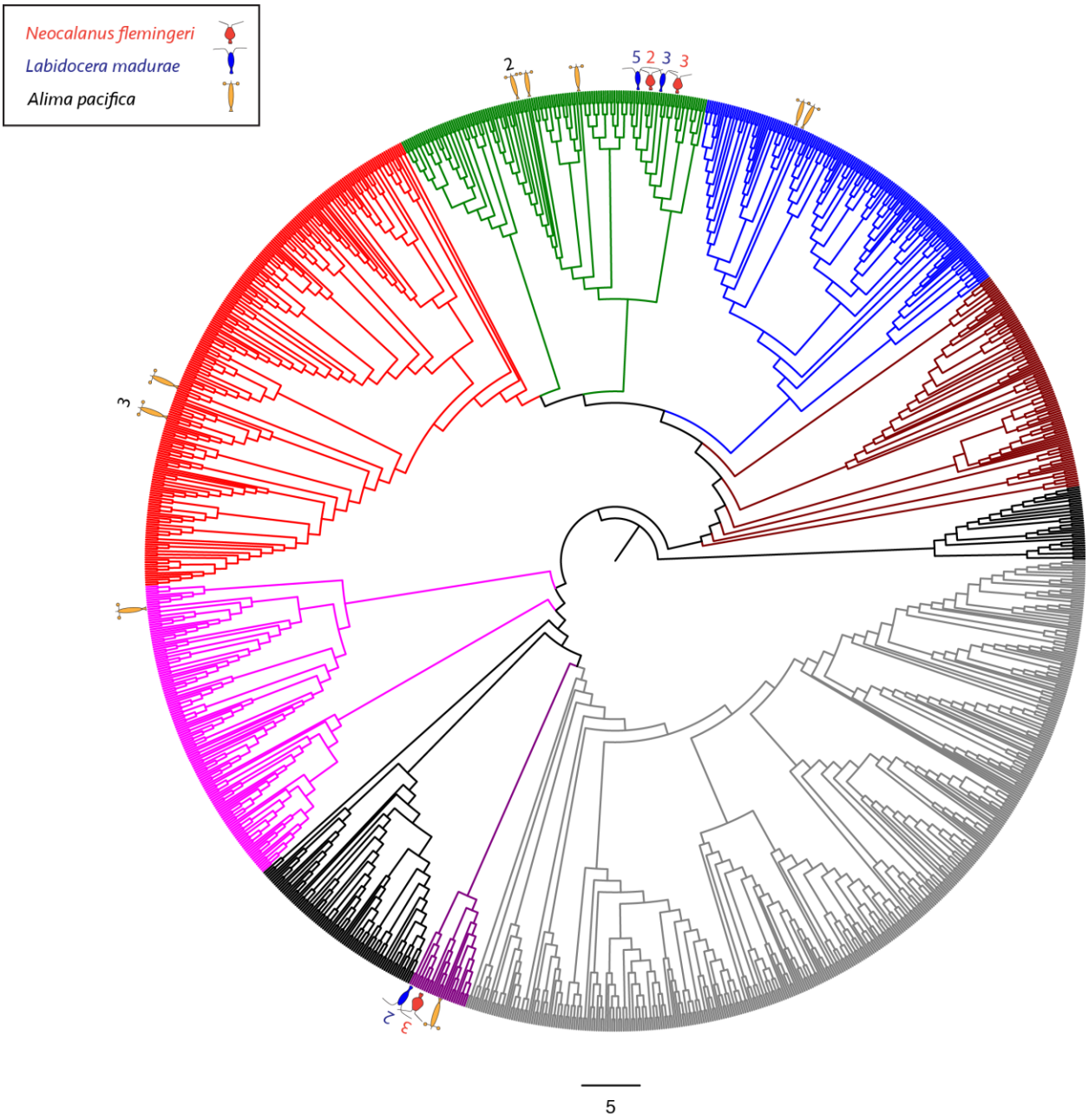

Figure 4.1 Maximum likelihood tree generated using CIPRES servers (UCSB, 2016) and RAxML algorithms. All opsins from Porter et al. (2012) and identified MWS opsins from Henze & Oakley (2015) were aligned using MUSCLE© algorithm, with regional realignments using ClustalW2. Opsin clades are colored as follows: gray – vertebrate c-type opsins, purple – invertebrate c-type opsins, black – cnidopsins, magenta – group 4 opsins, red – LWS opsins, green – MWS opsins, blue – SWS opsins, mahogany – basal r-type opsins. The outgroup rooting the tree consists of closely related GPCRs and is represented as the black colored clade between basal r-type opsins and c-type vertebrate opsins. Locations and numbers of contigs identified for *Neocalanus flemingeri, Labidocera madurae* and *Alima pacifica* are represented by colored symbols for each species with a corresponding number for the sequences identified, numbers not shown represent one sequence.

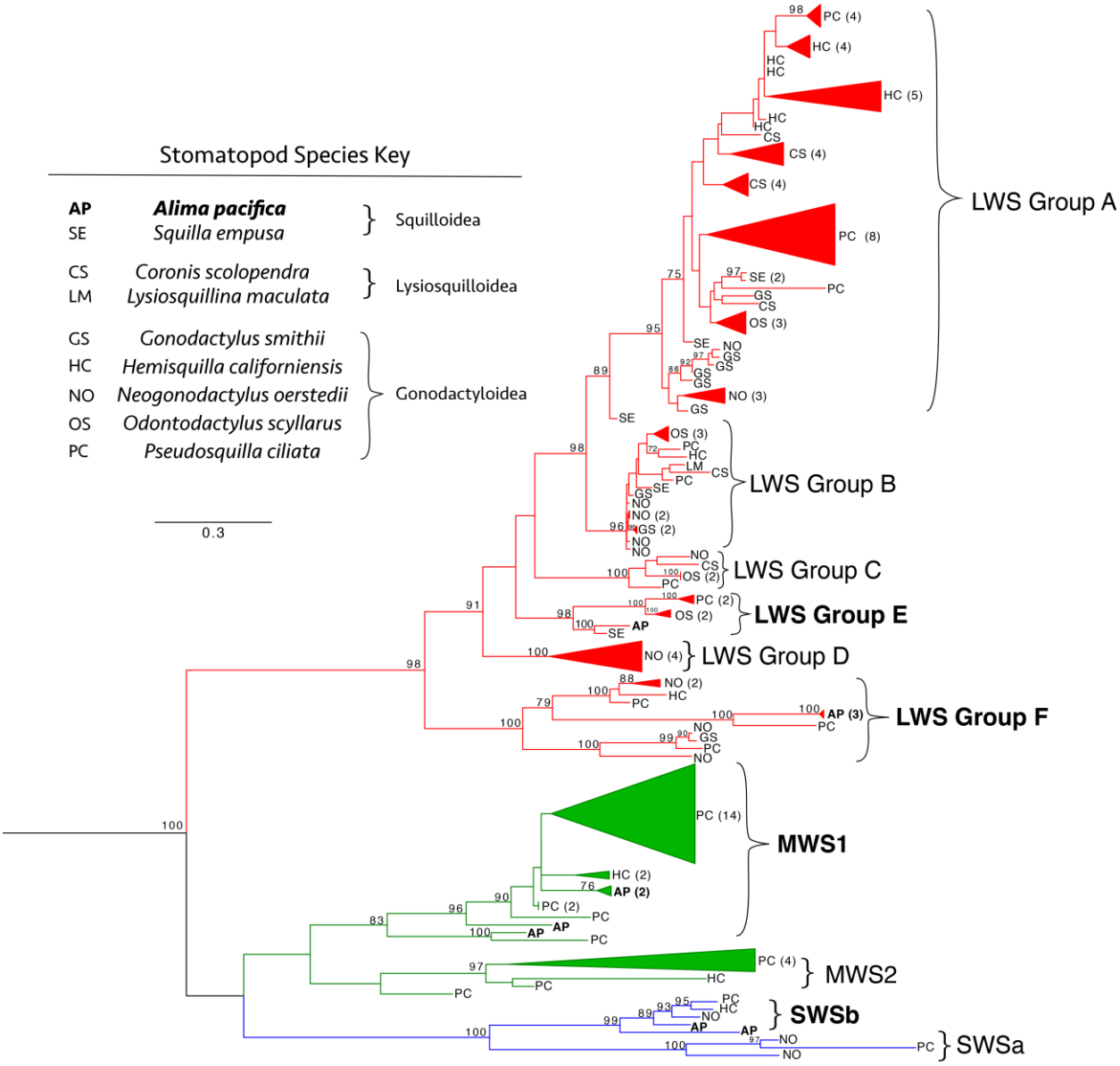

Figure 4.2 Maximum likelihood phylogeny of stomatopod r-type opsins from Porter et al. (2009) and Porter et al. (2013) with additional opsin protein sequences obtained from genbank for *Neogonodactylus oerstedii*. The tree was rooted using non-visual opsins from *Alima pacifica* (peropsin and pteropsin) and visual clades are color coded: LWS as red, MWS as green and SWS as blue. Clades were created based on previous groupings for LWS opsins from Porter et al. (2009) and for MWS and SWS groupings from Henze and Oakley (2015). Species names are abbreviated according to the key, and species are grouped by superfamily. Identified *Alima pacifica* opsins are found in bolded text groups.

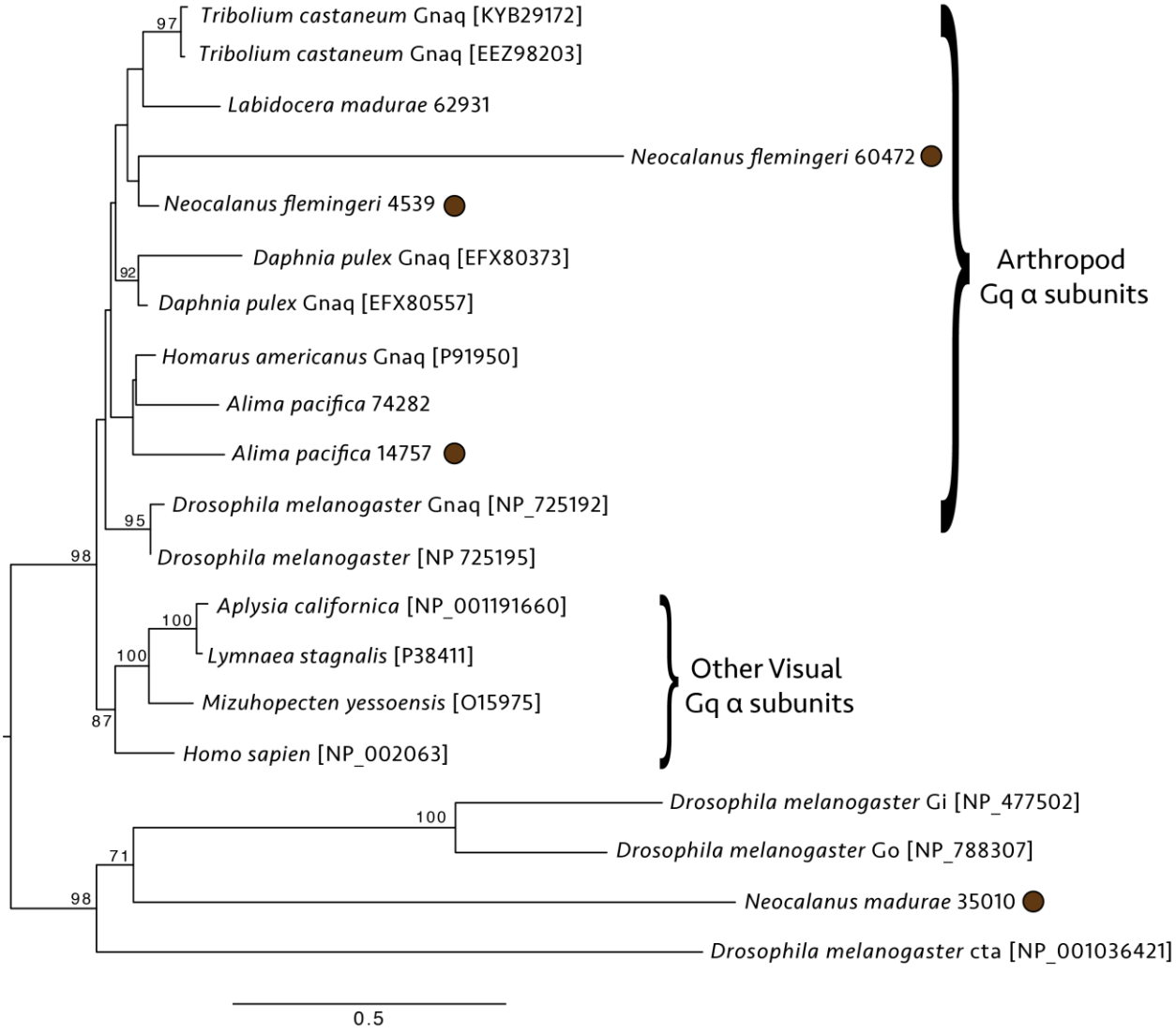

Figure 4.3 Gqα maximum likelihood phylogeny using sequences from the PIA workflow using other Gα subunits as an outgroup (Gi, Go, cta; Speiser et al., 2014). Trees were reconstructed from sequences which had been aligned using MUSCLE© on a CIPRES server using RAxML. Full length transcripts identified for *Alima pacifica*, *Labidocera madurae*, and *Neocalanus flemingeri* are represented as a brown circle after the sequence name. Bootstrap values greater than 70% are indicated on branches.

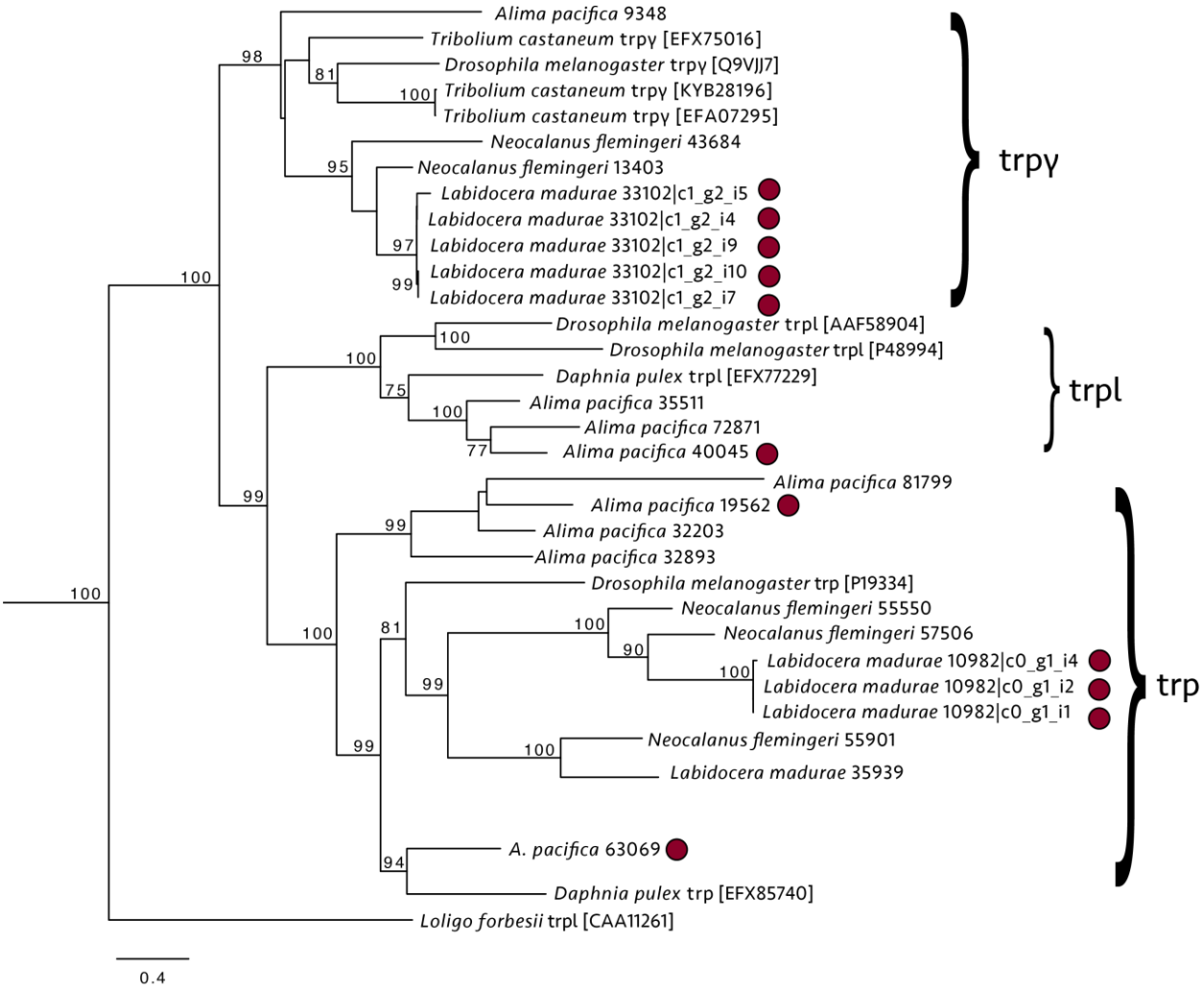

Figure 4.4 Maximum likelihood phylogeny of trp channels identified by PIA workflow aligned with visual trp proteins from invertebrates and *Homo sapien* (Speiser et al., 2014) using MUSCLE©. Phylogenies were reconstructed using RAxML on CIPRES servers (UCSB, 2016) and trp channel sequences from Homo sapiens were used as the outgroup (not shown here). Full length transcripts for *Alima pacifica*, *Labidocera madurae*, and *Neocalanus flemingeri* are represented as brown circles after the sequence name. Branches are labeled with bootstrap values (%) above 70.

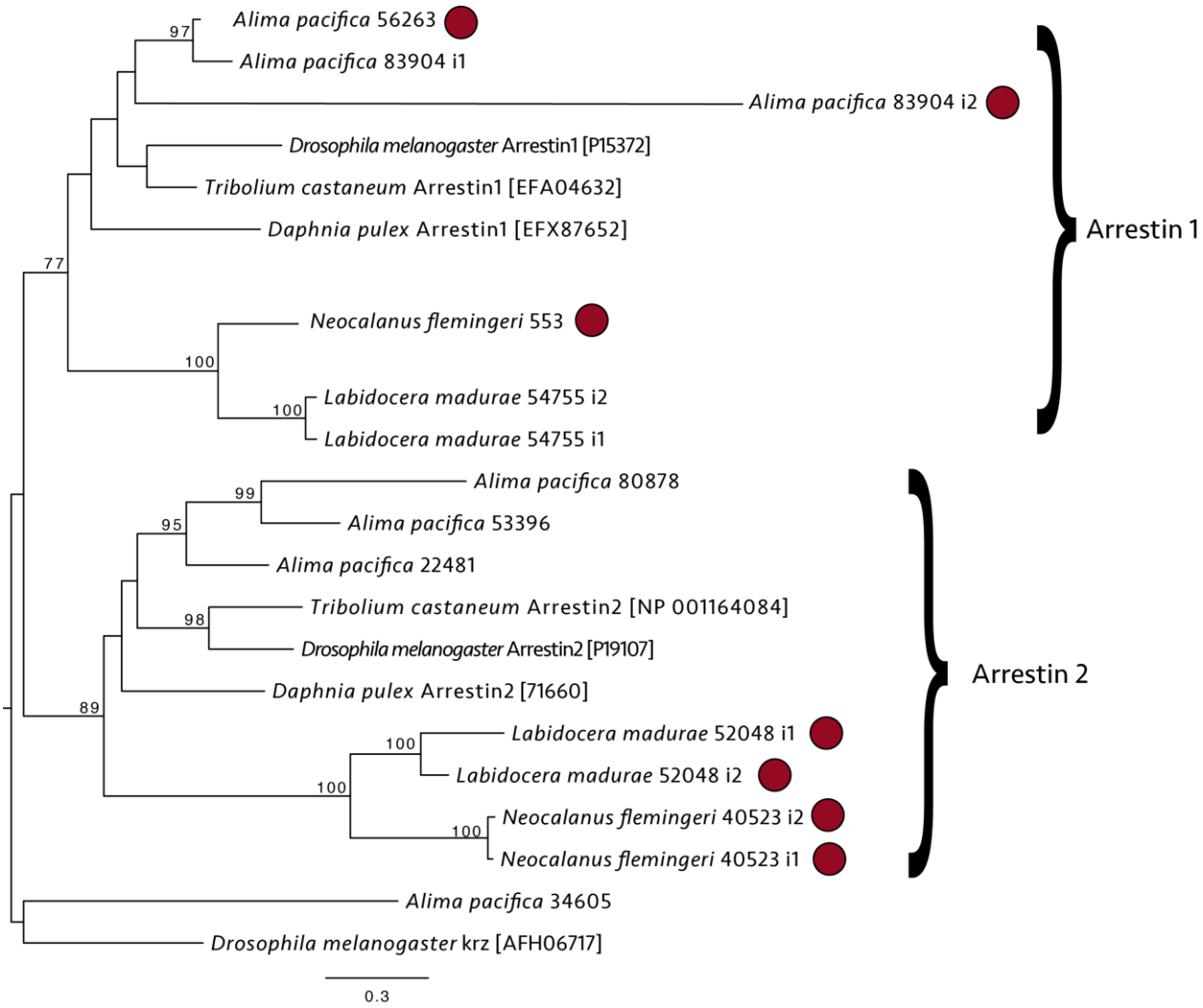

Figure 4.5 Arrestin phylogeny of visual arrestins from *D. melanogaster*, *Daphnia pulex*, and *Tribolium castaneum* with those identified for *L. madurae*, *N. flemingeri*, and *A. pacifica* from the PIA workflow (Speiser et al., 2014). Sequences were aligned using MUSCLE©, and a maximum likelihood phylogeny was reconstructed using RAxML on CIPRES servers (UCSB, 2016). Non-visual krz protein from *D. melanogaster* was used to root the tree. Full length transcripts are identified with a brown circle for *Alima pacifica*, *Labidocera madurae*, and *Neocalanus flemingeri*, with bootstrap values above 70% on the branches of the tree.

Appendix

Appendix A1 Table of contigs identified by PIA workflow as phototransduction genes. The nearest landmark sequence and accession number are identified for each transcript.

Contig ID	Landmark Sequence
TR81924|c0_g1_i1	SWS opsin
TR12918|c1_g1_i1	SWS opsin
TR15021|c0_g1_i1	MWS opsin
TR75868|c0_g1_i1	MWS opsin
TR49639|c3_g1_i2	MWS opsin
TR49639|c3_g2_i1	MWS opsin
TR28205|c0_g1_i3	LWS opsin
TR28205|c0_g1_i2	LWS opsin
TR28205|c0_g1_i1	LWS opsin
TR62817|c2_g1_i1	LWS opsin
TR54745|c0_g1_i1	Peropsin
TR69671|c0_g1_i1	Pteropsin
TR34605|c0_g1_i1	Arr 1 [P15372]
TR83904|c0_g1_i3	Arr 1 [P15372]
TR56263|c0_g4_i1	Arr 1 [P15372]
TR83904|c0_g2_i1	Arr 1 [P15372]
TR14326|c0_g1_i1	Arr2 [P19107]
TR19174|c0_g1_i1	Arr2 [P19107]
TR53396|c0_g1_i2	Arr2 [P19107]
TR80878|c0_g1_i1	Arr2 [P19107]
TR43029|c0_g1_i2	Arr2 [P19107]
TR22481|c0_g1_i1	Arr2 [P19107]
TR39836|c1_g2_i3	Gβ13F [P26308]
TR39836|c1_g2_i2	Gβ13F [P26308]
TR39836|c1_g2_i1	Gβ13F [P26308]
TR39836|c1_g1_i1	Gβ13F [P26308]
TR39836|c1_g2_i7	Gβ13F [P26308]
TR39836|c1_g2_i6	Gβ13F [P26308]
TR79326|c0_g1_i1	Gβ2 [XP 0018631]
TR62998|c0_g1_i2	Gβ2 [XP 0018631]
TR51899|c2_g1_i1	Gβ2 [XP 0018631]
TR51899|c2_g1_i2	Gβ2 [XP 0018631]
TR74282|c0_g1_i2	Gnαq [P91950]
TR14757|c2_g1_i1	Gnαq [P91950]
TR59997|c0_g1_i2	Gnαq [O15975]
TR59997|c0_g1_i1	Gnαq [O15975]
TR8633|c0_g2_i1	Gqγ30A [Q9NFZ3]
TR81640|c0_g1_i1	Gprk1 [P32865]
TR27483|c1_g2_i2	Gprk2 [P32866]
TR27483|c1_g2_i1	Gprk2 [P32866]
TR22581|c0_g1_i2	inaC [P13677]
TR56435|c0_g1_i6	norpA [P13217]
TR56435|c0_g1_i3	norpA [P13217]
TR56435|c0_g1_i2	norpA [P13217]
TR56435|c0_g1_i4	norpA [P13217]
TR56435|c0_g1_i1	norpA [P13217]
TR80857|c0_g1_i1	rdgA [Q09103]
TR80857|c0_g1_i4	rdgA [Q09103]
TR80857|c0_g1_i8	rdgA [Q09103]
TR80857|c0_g1_i7	rdgA [Q09103]
TR80857|c0_g1_i2	rdgA [Q09103]
TR80857|c0_g1_i9	rdgA [Q09103]
TR80857|c0_g1_i5	rdgA [Q09103]
TR80857|c0_g1_i3	rdgA [Q09103]
TR51878|c0_g1_i1	rdgA [XP 396522]
TR51878|c0_g1_i2	rdgA [XP 396522]
TR56211|c4_g4_i1	rdgB [P43125]
TR56211|c4_g6_i9	rdgB [P43125]
TR56211|c4_g6_i8	rdgB [P43125]
TR56211|c4_g6_i6	rdgB [P43125]
TR56211|c4_g6_i10	rdgB [P43125]
TR56211|c4_g6_i7	rdgB [P43125]
TR81799|c0_g1_i1	trp [P19334]
TR32203|c0_g1_i1	trp [P19334]
TR32893|c0_g1_i1	trp [P19334]
TR63069|c0_g1_i2	trp [P19334]
TR63069|c0_g1_i1	trp [P19334]
TR63069|c0_g1_i3	trp [P19334]
TR19562|c0_g3_i1	trp [P19334]
TR9348|c0_g1_i1	trpγ [Q9Vjj7]
TR35511|c0_g1_i1	trpl [P48994]
TR72871|c0_g1_i1	trpl [P48994]
TR40045|c1_g1_i1	trpl [P48994]

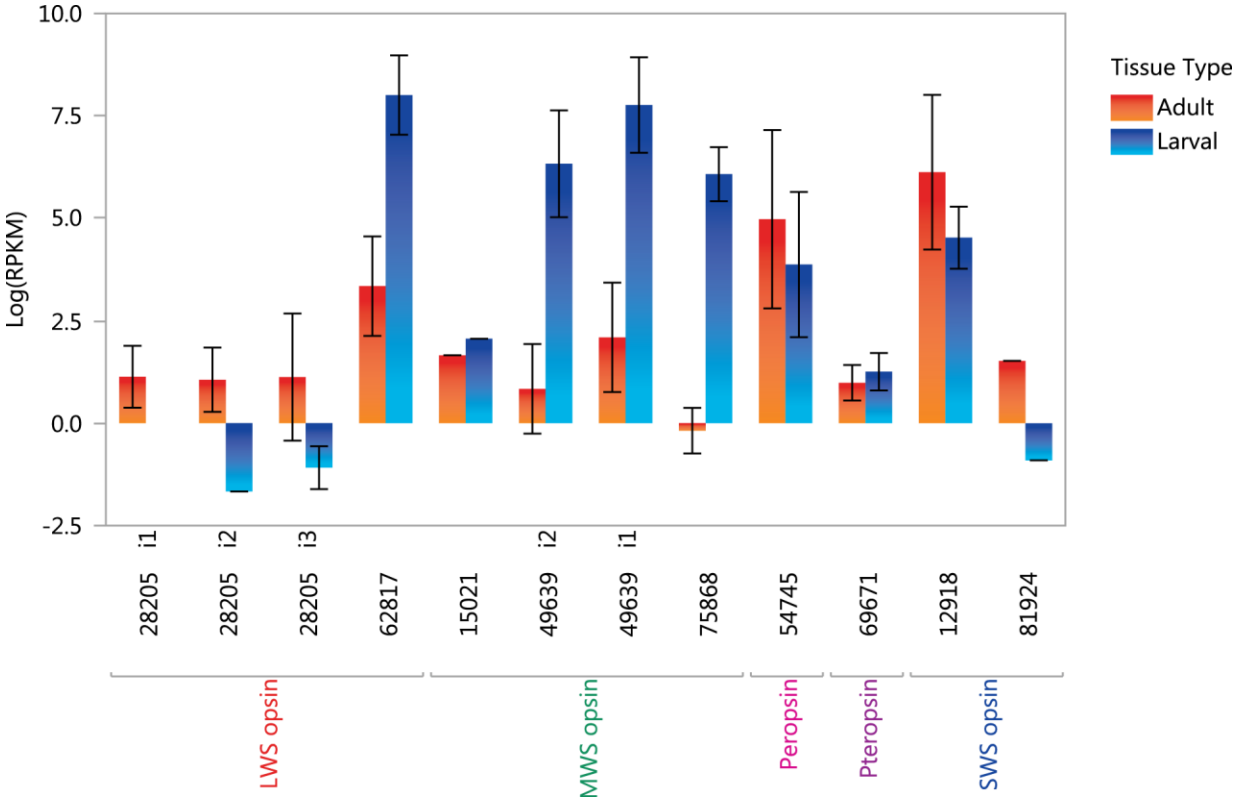

Appendix A2 Average expression in $\log_{10}$(RPKM) of opsin transcripts grouped by wavelength sensitive classes identified in *Alima pacifica*. Adult expression (blue) is compared to larval expression (red) for each transcript expressed. Error bars were constructed using one standard error from the mean square of opsin averages.

Literature Cited

Arendt, D., Tessmar-raible, K., Snyman, H., Dorresteijn, A.W., Wittbrodt, J., 2004. Ciliary photoreceptors with a vertebrate-type opsin in an invertebrate brain. Science (80-.). 306, 869–871.

Bellingham, J., Wilkie, S.E., Morris, A.G., Bowmaker, J.K., Hunt, D.M., 1997. Characterisation of the ultraviolet-sensitive opsin gene in the honey bee, Apis mellifera. Eur. J. Biochem. 243, 775–781. doi:10.1111/j.1432-1033.1997.00775.x

Bok, M.J., Porter, M.L., Place, A.R., Cronin, T.W., 2014. Biological sunscreens tune polychromatic ultraviolet vision in mantis shrimp. Curr. Biol. 24, 1636–1642. doi:10.1016/j.cub.2014.05.071

Briscoe, A.D., 2000. Functional diversification of lepidopteran opsins following gene duplication. Mol. Biol. Evol. 18, 2270–2279.

Buskey, E.J., Swift, E., 1985. Behavioral responses of oceanic zooplankton to simulated bioluminescence. Biol. Bull. 168, 263–275.

Cohen, J.H., Forward, R.B., 2002. Spectral sensitivity of vertically migrating marine copepods. Biol. Bull. 203, 307–314.

Colbourne, J.K., Pfrender, M.E., Gilbert, D., Thomas, W.K., Tucker, A., Oakley, T.H., Tokishita, S., Aerts, A., Arnold, G.J., Basu, M.K., Bauer, D.J., Cáceres, C.E., Carmel, L., Casola, C., Choi, J.-H., Detter, J.C., Dong, Q., Dusheyko, S., Eads, B.D., Fröhlich, T., Geiler-Samerotte, K.A., Gerlach, D., Hatcher, P., Jogdeo, S., Krijgsveld, J., Kriventseva, E. V., Kültz, D., Laforsch, C., Lindquist, E., Lopez, J., Manak, J.R., Muller, J., Pangilinan, J., Patwardhan, R.P., Pitluck, S., Pritham, E.J., Rechtsteiner, A., Rho, M., Rogozin, I.B., Sakarya, O., Salamov, A., Schaack, S., Shapiro, H., Shiga, Y., Skalitzky, C., Smith, Z., Souvorov, A., Sung, W., Tang, Z., Tsuchiya, D., Tu, H., Vos, H., Wang, M., Wolf, Y.I., Yamagata, H., Yamada, T., Ye, Y., Shaw, J.R., Andrews, J., Crease, T.J., Tang, H., Lucas, S.M., Robertson, H.M., Bork, P., Koonin, E. V., Zdobnov, E.M., Grigoriev, I. V., Lynch, M., Boore, J.L., 2011. The ecoresponsive genome of Daphnia pulex. Science 331, 555–561. doi:10.1126/science.1197761

Conover, R.J., Bedo, A.W., Herman, A.W., Harris, L.R., Horne, E.W., 1988. Never trust a copepod - some observations on their behavior in the Canadian Arctic. Bull. Mar. Sci. 43, 650–662.

Cronin, T., Bok, M., 2014. Filtering and polychromatic vision in mantis shrimps: themes in visible and ultraviolet vision. Philos. Trans. R. Soc. Lond. B. Biol. Sci. 396, 1–11.

Cronin, T.W., Jinks, R.N., 2001. Ontogeny of vision in marine crustaceans. Am. Zool. 41, 1098–1107. doi:10.1668/0003-1569(2001)041[1098:OOVIMC]2.0.CO;2

Cronin, T.W., Marshall, N.J., 1989. A retina with at least ten spectral types in a mantis shrimp. Nature 339, 137–140.

Cronin, T.W., Marshall, N.J., Caldwell, R.L., 1996. Visual pigment diversity in two genera of mantis shrimps implies rapid evolution (Crustacea; Stomatopoda). J. Comp. Physiol. A 179, 371–384. doi:10.1007/BF00194991

Cronin, T.W., Marshall, N.J., Caldwell, R.L., 1993. Photoreceptor spectral diversity in the retinas of squilloid and lysiosquilloid stomatopod crustaceans. J. Comp. Physiol. A Neuroethol. Sensory, Neural, Behav. Physiol. 172, 339–350.

Cronin, T.W., Porter, M.L., 2008. Exceptional Variation on a Common Theme : The Evolution of Crustacean Compound Eyes. Evol. Educ. Outreach 1, 463–475. doi:10.1007/s12052-008-0085-0

Cronin, T.W., Porter, M.L., Bok, M.J., Wolf, J.B., Robinson, P.R., 2010. The molecular genetics and evolution of colour and polarization vision in stomatopod crustaceans. Ophthalamic Physiol. Opt. 30, 460–469. doi:10.1111/j.1475-1313.2010.00762.x

Edgar, R.C., 2004. MUSCLE: Multiple sequence alignment with high accuracy and high throughput. Nucleic Acids Res. 32, 1792–1797. doi:10.1093/nar/gkh340

Elofsson, R., 2006. The frontal eyes of crustaceans. Arthropod Struct. Dev. 35, 275–291. doi:10.1016/j.asd.2006.08.004

Eriksson, B.J., Fredman, D., Steiner, G., Schmid, A., 2013. Characterisation and localisation of the opsin protein repertoire in the brain and retinas of a spider and an onychophoran. BMC Evol. Biol. 13, 1–10. doi:10.1186/1471-2148-13-186

Feiler, R., Bjornson, R., Kirschfeld, K., Mismer, D., Rubin, G., Smith, D., Socolich, M., Zuker, C., 1992. Ectopic expression of ultraviolet-rhodopsins in the blue photoreceptor cells of Drosophila: visual physiology and photochemistry of transgenic animals. J. Neurosci. 12, 3862–3868.

Feller, K.D., Cohen, J.H., Cronin, T.W., 2014. Seeing double : visual physiology of double - retina eye ontogeny in stomatopod crustaceans. J. Comp. Physiol. A 201, 331–339. doi:10.1007/s00359-014-0967-2

Feller, K.D., Cronin, T.W., 2016. Spectral absorption of visual pigments in stomatopod larval photoreceptors. J. Comp. Physiol. A 1–9. doi:10.1007/s00359-015-1063-y

Feller, K.D., Cronin, T.W., 2014. Hiding opaque eyes in transparent organisms: a potential role for larval eyeshine in stomatopod crustaceans. J. Exp. Biol. 217, 3263–3273. doi:10.1242/jeb.108076

Feller, K.D., Cronin, T.W., Ahyong, S.T., Porter, M.L., 2013. Morphological and molecular description of the late-stage larvae of Alima Leach, 1817 (Crustacea: Stomatopoda) from Lizard Island, Australia. Zootaxa 3722, 22–32.

Franke, R.R., König, B., Sakmar, T.P., Khorana, H.G., Hofmann, K.P., 1990. Rhodopsin mutants that bind but fail to activate transducin. Science (80-.). 250, 123–125. doi:10.1126/science.2218504

Hardie, R.C., Minke, B., 1992. The trp gene is essential for a light- activated Ca2 + channel in Drosophila photoreceptors. Neuron 8, 643–651. doi:10.1016/0896-6273(92)90086-S

Henze, M.J., Oakley, T.H., 2015. The dynamic evolutionary history of Pancrustacean eyes and opsins. Integr. Comp. Biol. 55, 1–13. doi:10.1093/icb/icv100

Kashiyama, K., Seki, T., Numata, H., Goto, S.G., 2009. Molecular characterization of visual pigments in Branchiopoda and the evolution of opsins in Arthropoda. Mol. Biol. Evol. 26, 299–311. doi:10.1093/molbev/msn251

Katz, B., Minke, B., 2009. Drosophila photoreceptors and signaling mechanisms. Front. Cell. Neurosci. 3, 1–18. doi:10.3389/neuro.03.002.2009

Kitamoto, J., Sakamoto, K., Ozaki, K., Mishina, Y., Arikawa, K., 1998. Two visual pigments in a single

photoreceptor cell : identification and histological localization of three mRNAS encoding visual pigment opsins in the retina of the butterfly Papilio xuthus. J. Exp. Biol. 201, 1255–1261.

Kobari, T., Ikeda, T., 2001. Life cycle of Neocalanus flemingeri (Crustacea: Copepoda) in the Oyashio region western subarctic Pacific, with notes on its regional variations. Mar. Ecol. Prog. Ser. 209, 243–255. doi:10.3354/meps209243

König, B., Arendt, A., McDowell, J.H., Kahlert, M., Hargrave, P.A., Hofmann, K.P., 1989. Three cytoplasmic loops of rhodopsin interact with transducin. Proc. Natl. Acad. Sci. 86, 6878–82.

Lacalli, T.C., 2009. Serial EM analysis of a copepod larval nervous system : naupliar eye, optic circuitry, and prospects for full CNS reconstruction. Arthropod Struct. Dev. 38, 361–375. doi:10.1016/j.asd.2009.04.002

Land, M.F., 1988. The functions of eye and other body movements in Labidocera and other Copepods. J. Exp. Biol. 140, 381–391.

Larkin, M.A., Blackshields, G., Brown, N.P., Chenna, R., Mcgettigan, P.A., McWilliam, H., Valentin, F., Wallace, I.M., Wilm, A., Lopez, R., Thompson, J.D., Gibson, T.J., Higgins, D.G., 2007. Clustal W and Clustal X version 2.0. Bioinformatics 23, 2947–2948. doi:10.1093/bioinformatics/btm404

Lenz, P.H., Roncalli, V., Hassett, R.P., Wu, L., Cieslak, M.C., Hartline, D.K., Christie, A.E., 2014. De novo assembly of a transcriptome for Calanus finmarchicus (Crustacea, Copepoda) – the dominant zooplankter of the North Atlantic Ocean. PLoS One 9, e88589. doi:10.1371/journal.pone.0088589

Machida, R.J., Tsuda, A., 2010. Dissimilarity of species and forms of planktonic Neocalanus copepods using mitochondrial COI , 12S , nuclear ITS , and 28S Gene Sequences. PLoS One 5, 1–6. doi:10.1371/journal.pone.0010278

Mackas, D.L., Louttit, G.C., 1988. Aggregation of the copepod Neocalanus plumchrus at the margin of the Fraser River plume in the Strait of Georgia. Bull. Mar. Sci. 43, 810–824.

Mahato, S., Morita, S., Tucker, A.E., Liang, X., Jackowska, M., Friedrich, M., Shiga, Y., Zelhof, A.C., 2014. Common transcriptional mechanisms for visual photoreceptor cell differentiation among Pancrustaceans. PLoS Genet. 10, e1004484. doi:10.1371/journal.pgen.1004484

Marshall, N.J., Cronin, T.W., Kleinlogel, S., 2007a. Stomatopod eye structure and function: A review. Arthropod Struct. Dev. doi:10.1016/j.asd.2007.01.006

Marshall, N.J., Cronin, T.W., Kleinlogel, S., 2007b. Stomatopod eye structure and function: A review. Arthropod Struct. Dev. 36, 420–448. doi:10.1016/j.asd.2007.01.006

Mojena, R., 1977. Hierarchical grouping methods and stopping rules: an evaluation. Comput. J. 20, 359–363. doi:10.1093/comjnl/20.4.359

Mortazavi, A., Williams, B.A., Mccue, K., Schaeffer, L., Wold, B., 2008. Mapping and quantifying mammalian transcriptomes by RNA-Seq. Nature 5, 621–628. doi:10.1038/NMETH.1226

Nagata, T., Koyanagi, M., Tsukamoto, H., Terakita, A., 2010. Identification and characterization of a protostome homologue of peropsin from a jumping spider. J. Comp. Physiol. A 196, 51–59. doi:10.1007/s00359-009-0493-9

Niemeyer, B.A., Suzuki, E., Scott, K., Jalink, K., Zuker, C.S., 1996. The Drosophila light-activated conductance is composed of the two channels TRP and TRPL. Cell 85, 651–659. doi:10.1016/S0092-8674(00)81232-5

Nilsson, D.-E., 2013. Eye evolution and its functional basis. Vis. Neurosci. 30, 5–20. doi:10.1017/S0952523813000035

Oakley, T.H., Huber, D.R., 2004. Differential expression of duplicated opsin genes in two eye types of Ostracod Crustaceans. J. Mol. Evol. 59, 239–249. doi:10.1007/s00239-004-2618-7

Ohtsuka, S., Huys, R., 2001. Sexual dimorphism in calanoid copepods : morphology and function. Hydrobiologia 453, 441–466.

Passamaneck, Y.J., Furchheim, N., Hejnol, A., Martindale, M.Q., Lüter, C., 2011. Ciliary photoreceptors in the cerebral eyes of a protostome larva. Evodevo 2, 6. doi:10.1186/2041-9139-2-6

Pearn, M.T., Randall, L.L., Shortridge, R.D., Burg, M.G., Pak, W.L., 1996. Molecular, biochemical , and electrophysiological characterization of Drosophila norpA mutants. J. Biol. Chem. 271, 4937–4945.

Peterson, W.T., 2001. Patterns in stage duration and development among marine and freshwater calanoid and cyclopoid copepods : a review of rules , physiological constraints , and evolutiona ... constraints , and evolutionary significance. Hydrobiologia 453/454, 91–105. doi:10.1023/A

Porter, M.L., Blasic, J.R., Bok, M.J., Cameron, E.G., Pringle, T., Cronin, T.W., Robinson, P.R., 2012. Shedding new light on opsin evolution. Proc. R. Soc. B Biol. Sci. 279, 3–14. doi:10.1098/rspb.2011.1819

Porter, M.L., Bok, M.J., Robinson, P.R., Cronin, T.W., 2009. Molecular diversity of visual pigments in Stomatopoda (Crustacea). Vis. Neurosci. 26, 255–265. doi:10.1017/S0952523809090129

Porter, M.L., Speiser, D.I., Zaharoff, A.K., Caldwell, R.L., Cronin, T.W., Oakley, T.H., 2013. The evolution of complexity in the visual systems of Stomatopods : insights from transcriptomics. Integr. Comp. Biol. 53, 39–49. doi:10.1093/icb/ict060

Porter, M.L., Zhang, Y., Desai, S., Caldwell, R.L., Cronin, T.W., 2010. Evolution of anatomical and physiological specialization in the compound eyes of stomatopod crustaceans. J. Exp. Biol. 213, 3473–3486. doi:10.1242/jeb.046508

Prete, F.R., 2004. Complex worlds from simpler nervous systems. MIT Press.

Rajkumar, P., Rollmann, S.M., Cook, T.A., Layne, J.E., 2010. Molecular evidence for color discrimination in the Atlantic sand fiddler crab, Uca pugilator. J. Exp. Biol. 213, 4240–4248. doi:10.1242/jeb.051011

Randel, N., Bezares-Calderón, L. a, Gühmann, M., Shahidi, R., Jékely, G., 2013. Expression dynamics and protein localization of rhabdomeric opsins in Platynereis larvae. Integr. Comp. Biol. 53, 7–16. doi:10.1093/icb/ict046

Roncalli, V., Cieslak, M.C., Passamaneck, Y., Christie, A.E., 2015. Glutathione S-Transferase (GST) gene diversity in the Crustacean Calanus finmarchicus – contributors to cellular detoxification. PLoS One 10, 1–27. doi:10.1371/journal.pone.0123322

Sakamoto, K., Hisatomi, O., Tokunaga, F., Eguchi, E., 1996. Two opsins from the compound eye of the crab Hemigraspus sanguineus. J. Exp. Biol. 199, 441–450.

Schönenberger, N., 1977. The fine structure of the compound eye of Squilla mantis (Crustacea, Stomatopoda). Cell Tissue Res. 176, 205–233.

Speiser, D.I., Pankey, M., Zaharoff, A.K., Battelle, B.A., Bracken-Grissom, H.D., Breinholt, J.W., Bybee, S.M., Cronin, T.W., Garm, A., Lindgren, A.R., Patel, N.H., Porter, M.L., Protas, M.E., Rivera, A.S., Serb, J.M., Zigler, K.S., Crandall, K.A., Oakley, T.H., 2014. Using phylogenetically-informed annotation (PIA) to search for light-interacting genes in transcriptomes from non-model organisms. BMC Bioinformatics 15, 350. doi:10.1186/s12859-014-0350-x

Sun, H., Gilbert, D.J., Copeland, N.G., Jenkins, N.A., Nathans, J., 1997. Peropsin , a novel visual pigment-like protein located in the apical microvilli of the retinal pigment epithelium. Proc. Natl. Acad. Sci. 94, 9893–9898.

Suzuki, E., Masai, I., Inoue, H., Awasaki, T., 2003. The neural basis of early vision. Springer Japan, Tokyo. doi:10.1007/978-4-431-68447-3_34

Townson, S.M., Chang, B.S., Salcedo, E., Chadwell, L. V., Pierce, N.E., Britt, S.G., 1998. Honeybee blue- and ultraviolet-sensitive opsins: cloning, heterologous expression in Drosophila, and physiological characterization. J. Neurosci. 18, 2412–2422.

Tsuda, A., Saito, H., Kasai, H., 1999. Life histories of Neocalanus flemingeri and Neocalanus plumchrus (Calanoida : Copepoda) in the western subarctic Pacific. Mar. Biol. 135, 533–544.

Velarde, R.A., Sauer, C.D., Walden, K.K., Fahrbach, S.E., Robertson, H.M., 2005. Pteropsin: A vertebrate-like non-visual opsin expressed in the honey bee brain. Insect Biochem. Mol. Biol. 35, 1367–1377. doi:10.1016/j.ibmb.2005.09.001

Waggett, R.J., Buskey, E.J., 2007. Calanoid copepod escape behavior in response to a visual predator. Mar. Biol. 150, 599–607. doi:10.1007/s00227-006-0384-3

Wakakuwa, M., Terakita, A., Koyanagi, M., Stavenga, D.G., Shichida, Y., Arikawa, K., 2010. Evolution and mechanism of spectral tuning of Blue-absorbing visual pigments in butterflies. PLoS One 5, 1–8. doi:10.1371/journal.pone.0015015

Warrant, E., Nilsson, D.-E., 2006. Invertebrate vision. Cambridge University Press.

Williams, B.G., Greenwood, J.G., Jillett, J.B., 1985. Seasonality and duration of the developmental stages of Heterosquilla tricarinata (Claus, 1871) (Crustacea: Stomatopoda) and the replacement of the larval eye at metamorphosis. Bull. Mar. Sci. 36, 104–114.